Reelin Controls the Directional Orientation, Apical Localization and Length of Primary Cilia in Principal Neurons in the Cerebral Cortex

Sumaya Akter[1], Soheila Mirhosseiniardakani[1], Yuto Takekoshi[3], Liyan Qiu[1], Kevin Baker[1], Kevin Jiang[1], Mark Lyon[2], Mitsuharu Hattori[3,*] and Xuanmao Chen[1,*]

[1]Department of Molecular, Cellular, and Biomedical Sciences; College of Life Sciences and Agriculture, University of New Hampshire, 46 College Road, Durham, NH 03824. [2]Department of Mathematics and Statistics, College of Engineering and Physical Sciences, University of New Hampshire, Durham, NH 03824. [3]Department of Biomedical Science, Graduate School of Pharmaceutical Sciences, Nagoya City University, Nagoya, Aichi 467-8603, Japan. *Correspondence should be addressed to Mitsuharu Hattori, email: mhattori@phar.nagoya-cu.ac.jp or Xuanmao Chen, email: Xuanmao.Chen@unh.edu

Running Title: Reelin Influences Ciliation Patterns

Key Words: Primary Cilia, Reelin, Postnatal Neuron Positioning, Cilia Orientation, Reverse Movement, Apical-Basal Neuron Polarity

Funding and Acknowledgments: This research was supported by National Institutes of Health Grants P20GM113131-7006, R15MH126317, and R15MH125305 to X.C.; and by UNH CoRE awards, Cole Neuroscience and Behavioral Faculty Research Awards, and a COLSA Community of Teaching and Research Scholar Award (to X.C.); Grants-in-aid for Scientific Research of Japan Society for Promotion of Science JP24KJ1889 to Y.T.; Grants-in-aid for Scientific Research of Japan Society for Promotion of Science JP20H03384 and JP23K27324 (to M.H).; Grant-in-Aid for Outstanding Research Group Support Program in Nagoya City University (Grant Number 2401101). S.A. and S.M. were funded by UNH Summer TA Research Fellowships (STAF), K.B. by a McNair Scholar Award, and K.J. by an Undergraduate Research Award at UNH. We are grateful to the University Instrumentation Center at UNH for A1R HD confocal imaging service.

Abstract

The primary cilia of pyramidal neurons in inside-out laminated regions orient predominantly toward the pial surface, reflecting reverse soma re-positioning during postnatal development. However, the mechanisms underlying the directional cilia orientation and reverse movement are unknown. Here we show that the primary cilia of pyramidal neurons are localized near the base of the apical dendrites and aligned on the nuclear side opposite to the axon initial segment. However, this pattern is not observed in atypical pyramidal neurons in the deep neocortex, excitatory neurons in non-laminated brain regions, interneurons, or astrocytes, where their cilia are irregularly positioned around the nuclei and lack preferred orientation. In Reelin-deficient mice (*reeler*), the directional orientation and apical localization of cilia in late-born neocortical and CA1 neurons are partially impaired, because their initial impairments are partially corrected during late postnatal development, along with a realignment of apical-basal orientation. In contrast, loss of Reelin drastically disrupts the directional orientation of primary cilia in early-born neocortical neurons and principal neurons in the piriform cortex; consistently, their cilia and centrioles do not preferably localize to the base of the apical dendrites. Additionally, Reelin deficiency increases the cilia length of principal neurons in the cerebral cortex after P14 when WT cilia stabilize, but not in interneurons, astrocytes, or excitatory neurons in non-laminated regions. Together, Reelin controls the directional orientation, intracellular localization, and length of primary cilia in principal neurons in the cerebral cortex. These results underscore primary cilia as a key apical unit, particularly prominent in late-born neurons.

Introduction

The extracellular matrix protein Reelin is a crucial determinator directing neuronal migration of principal neurons and lamina formation in the cerebral cortex (Alexander et al., 2023; Hattori, 2025; Jossin, 2020). Reelin exerts its effects through binding to two lipoprotein receptors, ApoER2 and VLDLR, initiating a signaling cascade involving the phosphorylation of the adaptor protein Dab1 (Frotscher et al., 2009; Trommsdorff et al., 1999). By modulating cytoskeleton dynamics, stabilizing leading process, and regulating terminal soma translocation (Jossin, 2020), Reelin influences the establishment and maintenance of apical-basal polarity of principal neurons in the cerebral cortex (Kupferman et al., 2014; Matsuki et al., 2010). Disruption of Reelin and its essential downstream signaling proteins, as seen in Reelin null mutant *reeler* (D'Arcangelo et al., 1995), ApoER2 and VLDLR double knockouts (Frotscher et al., 2009; Trommsdorff et al., 1999), and Dab1 null mutant mice (Howell et al., 1997; Sheldon et al., 1997; Yoneshima et al., 1997), results in abnormal neuronal morphology, apical-basal misorientation, and profoundly disorganized cortical formations. These changes are associated with numerous downstream consequences, including synaptic dysfunction and severe neurological disorders such as lissencephaly, ataxia, and schizophrenia and neurodegeneration (Alexander et al., 2023; Hattori, 2025; Ishii et al., 2016; Joly-Amado et al., 2023; Jossin, 2020; Katsuyama and Hattori, 2024; Stranahan et al., 2013). While Reelin is known to guide embryonic neuronal migration and cortical lamination (Alexander et al., 2023; Jossin, 2020; Katsuyama and Hattori, 2024), its impacts on postnatal neuronal positioning and underlying mechanisms are not fully understood.

Primary cilia are centriole-derived organelles that are expressed in nearly all mammalian cells, including neurons (Bishop et al., 2007; Sterpka and Chen, 2018; Wilsch-Bräuninger and Huttner, 2021;

Yang et al., 2025). Cilia length and ciliation frequency vary greatly across brain regions, developmental stages, day and night rhythm, as well as metabolic or disease conditions (Macarelli et al., 2023; Phua et al., 2019; Sterpka et al., 2020; Tu et al., 2023; Yang et al., 2025). Altered ciliary signaling affects neurodevelopment, leading to various ciliopathies such as cortical malformation, cognitive deficits, and behavioral abnormalities (Green and Mykytyn, 2014; Hasenpusch-Theil and Theil, 2021; Lee and Gleeson, 2011; Singla and Reiter, 2006). During embryonic neurodevelopment, primary cilia coordinate key signaling pathways such as the sonic hedgehog signaling (Bangs and Anderson, 2017; Breunig et al., 2008; Ho and Stearns, 2021) and WNT signaling (Niehrs et al., 2025; Vuong and Mlodzik, 2023), and regulate multiple developmental processes (Valente et al., 2014), including cell fate determination (Jang et al., 2016; Yanardag and Pugacheva, 2021) and dorsal-ventral patterning of the neural tube (Pal and Mukhopadhyay, 2015; Sasai and Briscoe, 2012). However, specifically the primary cilia of principal neurons in the cerebral cortex do not fully arise during the embryonic stage (Yang et al., 2025). The emanation of primary cilia out of the centrioles that occurs postnatally, varying from P3 to P14, depending on animal strains and brain regions, may reflect the dynamic process of postnatal neuron positioning. We have previously analyzed cilia morphology and directionality in the postnatal mouse cerebral cortex and found that after postnatal day 14 (P14), the primary cilia of principal neurons in inside-out laminated brain regions spanning from the hippocampal CA1 region to neocortex are predominantly oriented toward the pial surface (Yang et al., 2025). Along with other converging evidence, the directional orientation of cilia reflects a slow “reverse movement” of late-born pyramidal neurons during postnatal positioning (Yang et al., 2025).

In this study, we initially found that the primary cilia of principal neurons, particularly late-born pyramidal neurons, in the cerebral cortex are localized to the base of the apical dendrites, aligning opposite to the axon initial segment in reference to the nucleus. However, this phenomenon is not

observed in atypical pyramidal neurons in the deep neocortex, excitatory neurons in nucleated brain regions, interneurons, or astrocytes. Yet, it is unknown which factor controls the cilia directionality and apical localization in principal neurons in the cerebral cortex. Given Reelin guides neuronal migration and strongly influences the neuronal polarity of pyramidal neurons (D'Arcangelo et al., 1995; Kupferman et al., 2014; Matsuki et al., 2010), we tested the hypothesis that Reelin dictates cilia orientation and cilia apical localization in principal neurons. Using Reelin null mice (*reeler*) (Curran et al., 1995; D'Arcangelo et al., 1995; Falconer, 1951; Ogawa et al., 1995), we discovered that Reelin impacts cilia directional orientation and cilia localization to the base of apical dendrites of pyramidal neurons in the cerebral cortex. Surprisingly, Reelin deficiency affects early-born neurons and principal neurons in the piriform cortex more severely than late-born principal neurons with respect to cilia orientation, cilia apical localization and apical-basal neuronal orientation. In addition, Reelin deficiency also promotes cilia elongation in principal neurons throughout the laminated cerebral cortex after P14, when WT cilia stabilize (Yang et al., 2025). However, Reelin does not affect cilia length in interneurons, astrocytes, or excitatory neurons in nucleated brain regions. In conclusion, Reelin controls the directional orientation, apical localization, and length of primary cilia in principal neurons in the cerebral cortex. These data also suggest that primary cilia represent a key apical component of pyramidal neurons, and late-born neurons exhibit special features in postnatal positioning, cilia localization and apical-basal orientation, which are absent in early-born neurons or evolutionarily older neurons.

Methods and Materials

Animals

Mice were housed under a 12-hour light/dark cycle (lights on from 6:00 A.M. to 6:00 P.M.) and provided with standard chow and water ad libitum. Crl:CD-1 mice (RRID: MGI:5652673) were obtained from Japan SLC. *Reeler* mice (B6C3Fe a/a-Reln^{rl} /J, RRID: IMSR_JAX:000235) were obtained from the Jackson Laboratory and backcrossed to the Crl:CD-1 strain. Both male and female mice were used in all experiments. Mice were fixed with 4% paraformaldehyde (PFA) in phosphate-buffered saline (PBS) by intracardiac perfusion. The brains were post-fixed with 4% PFA in PBS overnight before dehydration using 30% sucrose. If not otherwise indicated, experiments were performed using wild-type mice with C57BL/6j genetic background. All animal procedures were approved by the Institutional Animal Care and Use Committee of the University of New Hampshire (Approved Numbers: 191102 and 221202) or by the Animal Care and Use Committee of the Nagoya City University and conducted in accordance with the Institutional Guidelines for Animal Experimentation (Approval Number: 23-001H05).

Immunofluorescence Staining

Mouse brains were sliced and mounted on gelatin-coated slices for doing immunostaining method. They were washed three times with 0.1 M PBS. Then they were washed in 0.2% Triton X-100 (vol/vol) in 0.1 M PBS three times for 10 minutes at room temperature. Then they were blocked in blocking buffer (0.1M PBS containing 10% normal donkey serum (vol/vol), 2% bovine serum albumin (weight/vol), 0.2% Triton X-100 (vol/vol)) for 1-2 h at room temperature. After that, slices were incubated with primary antibodies overnight at 4 °C in blocking buffer. After washing in 0.1 M PBS three times for 10 minutes, slices were incubated with secondary antibodies for 2 hours at room temperature. Primary antibodies were rabbit anti-AC3 (1:10000 dilution, EnCor Biotechnology Inc., #RPCA AC3) or mouse anti-AC3 (1:1000 EnCor Biotechnology Inc., #MCA-1A12), Rabbit anti-Glutaminase I (1:500, Synaptic Systems #456003), rat anti-Ctip2 (1:500, Millipore-Sigma, MABE1045), rabbit anti-Satb2 (1:500,

Abcam, ab92446), mouse anti-Ankyrin G (1:500, Synaptic System, #181011), and mouse anti-NeuN (1:500, Millipore-Sigma, MAB377, clone A60). Secondary antibodies were mostly from Donkey conjugated with Alexa Fluor 488, 546, or 647 (Invitrogen, La Jolla, CA). Finally, sections were counter-stained with DAPI (Southern Biotech, #OB010020) and images were acquired with confocal microscope (Nikon, A1R-HD), installed in the University Instrument Center.

Cilia Orientation Measurement

Cilia orientation of early-born neurons was measured based on immunostaining of CTIP2 and AC3 antibodies. Cilia orientation of late-born neurons was measured based on immunostaining of Satb2 and AC3 antibodies. Cilia orientation of excitatory neurons was measured based on immunostaining of Glutaminase II and AC3 antibodies. GFAP and GAD65 antibodies were employed in immunostaining to differentiate astrocyte and interneurons. We used custom-made MATLAB Apps, named Cilia Locator and Cilia Analysis, to identify cilia in confocal images and determine cilia directionality (Yang et al., 2025) and (Mirhosseiniardakani et al., 2025 bioRxiv). Collected data were exported into Excel file and then to a MATLAB program, which was used to generate polar plots, histogram and fit histogram.

Primary Cilia Length Measurement

We assessed the primary cilia length following published methods (Sipos et al., 2018), with modifications. Cilia length was measured using the freehand line tool within Fiji (ImageJ) from the base of axoneme to the distal tip.

Cilia and Axon Quadrant Analysis

NeuN and Glutaminase II immunostaining revealed the shapes of apical dendrites of principal neurons, which allowed cilia localization analysis. To evaluate the spatial distribution of primary cilia and axons in various cell types and different brain regions, high-resolution confocal images were acquired using a

40X oil-immersion objective in Nikon's Confocal microscope. Each soma/cell body was subdivided into four quadrants like apical, basal, left lateral, and right lateral by drawing perpendicular lines in Fiji (ImageJ) intersecting at the center of nuclear centriole, aligned with the apical–basal axis of the neuron. For interneurons and astrocytes which may not aways have primary dendrites, we separate each soma into four quadrants (top, bottom, left lateral, and right lateral). Each cilium base (centriole) or axons position was determined based on the quadrant in which the majority of the ciliary axoneme was localized. For each location, a minimum of 100 cells per condition were analyzed across multiple sections and animals. The percentage of cilia/axon in each quadrant was calculated and compared to determine whether they were equally distributed among the four orientations.

Cilia Orientation Analysis Software and General Statistics

Data analysis was conducted using Fiji, GraphPad Prism and presented using CorelDRAW. A custom-made MATLAB Application was developed to analyze cilia orientation data. The software utilized MATLAB's custom distribution fitting algorithms to facilitate the fitting of the orientation data to several different distribution models (uniform distribution - irregular cilia orientation; mono periodic normal distribution - one major cilia orientation; and double periodic normal distribution - two cilia orientations). The Kolmogorov - Smirnov test was applied to test the hypothesis that sampled orientation distribution could have been drawn from the fit probability distribution and facilitated the plotting of both the sampled orientation distribution and fit probability distribution. General statistical analyses were conducted using an independent two-sample t-test to evaluate statistical significance between the WT and *reeler* groups, with a significance threshold of $p < 0.05$. Unless otherwise specified in the text or figure legends, significance levels are indicated as follows: ns (not significant); * $p < 0.05$; ** $p < 0.01$; *** $p < 0.001$. Statistical significance was determined in the graph at $p < 0.05$, with values

presented as mean ± standard error of the mean (SEM). Data were collected from multiple sections from three or more mice (mixed sex) for each group, if not otherwise indicated.

Results

Primary Cilia of Pyramidal Neurons in Inside-out Laminated Regions are Located Near the Base of Apical Dendrites.

To examine the spatial relationship between centrioles (or cilia base) localization, cilia orientation, and the apical dendrites in the WT neocortex, we performed immunofluorescence staining on fixed WT brain sections using AC3 antibodies, an established cilia marker, along with cell type-specific markers. We analyzed confocal images to systematically assess the orientation and intracellular localization of primary cilia in various cell types and brain regions. Firstly, cilia or centrioles are consistently localized near the base of the apical dendrites of pyramidal neurons in all inside-out laminated brain regions, which include the neocortex (except for atypical pyramidal neurons), entorhinal cortex, cingulate cortex, hippocampal CA1, and piriform cortex (Fig. 1A-B, Table 1). Intriguingly, the cilia or centriole intracellular localization is consistent with their cilia orientation predominantly toward the pial surface, align opposite to axon initial segment relative to the nuclei (Fig. 1C-D). We also compared principal neurons in superficial and deep cortical layers at P30. In both layers, the bases of cilia (centrioles) were mostly positioned near the base of the apical dendrite, with primary cilia projecting in the same pia direction. This alignment reflects a well-organized structural polarity, supporting the coordinated localization of subcellular organelles along the apical-basal axis in a properly laminated cortex. Notably, the pattern of cilia-at-apical while axon-at-basal is most striking in late-born neurons, compared to early-

born neurons and other cell types, in line with stronger cilia orientation toward the pial surface in late-neurons (Figure 1C-D).

Secondly, atypical pyramidal neurons in the deep neocortex, which are deviate from the classical morphological and electrophysiological features of pyramidal neurons (Landrieu and Goffinet, 1981), and some have inverted, while others have oblique apical dendrites (Steger et al., 2018; Steger et al., 2013). Immunostaining for AC3, Glutaminase II (or NeuN) and DAPI revealed abundant cilia in these cells (Fig. S1). However, cilia orientation showed an irregular pattern. The histogram of angular frequency demonstrated a broad, evenly dispersed distribution without dominant peak (Fig. S1D), suggesting a lack of preferred orientation. This was further confirmed by the cilia orientation map (Fig. S1C), which showed diverse angular values without regional clustering. The analysis of cilia localization (Fig. S1E) also revealed even distribution of cilia among four quadrants, further supporting the absence of localization bias. These results indicate that, unlike pyramidal neurons in laminated regions, atypical pyramidal neurons in the WT deep neocortical layer do not display specific cilia orientation.

Thirdly, pyramidal or excitatory neurons in the amygdala are laminated but organized into distinct nuclei (LeDoux, 2007). Their cilia distribution pattern somewhat resembled that of atypical pyramidal neurons in the deep neocortex: neuronal primary cilia do not preferably localize to the base of the apical dendrites (the apical quadrant) and cilia lack specific orientation (Fig. S2). Fourthly, in many other nucleated (or non-laminated) brain regions examined, such as hypothalamus, striatum, thalamus, cilia of excitatory neurons were randomly located in the soma near to the nuclei and no directional cilia orientation were detected (Table 1). Fifthly, cilia of interneurons and astrocytes throughout the brain were irregularly distributed within the cell body around the nucleus (Table 1) (Fig. S3) and their cilia did not exhibit a directional orientation (Yang et al., 2025). Together, the primary cilia of pyramidal neurons in inside-out laminated brain regions generally localize near the base of apical dendrites (the apical

quadrant) and predominantly orient toward the pial surface, while interneurons and astrocytes, atypical pyramidal neurons, and excitatory neuron in non-laminated regions do not manifest such a pattern.

Late-born, but Not Early-born Neocortical Neurons, Exhibit Postnatal Correction in Cilia Orientation and Cilia Apical Localization, Following Disruptions Caused by Reelin Deficiency.

Reelin is a key extracellular cue that influences neuronal placement, apical-basal neuronal polarity, and layering in the cerebral cortex (Jossin, 2020; Rice and Curran, 2001). To assess whether Reelin influences the cilia orientation of primary cilia of cortical pyramidal neurons, we examined cilia directionality in the outer layer of the neocortex in WT and *reeler* mice at P30. *Reeler* carries a mutation in the Reelin gene (*Reln*) and is an extensively characterized null model (D'Arcangelo et al., 1995). Immunofluorescence images show that in WT mice primary cilia exhibited a predominant orientation toward the pial surface (Fig. 2A). Quantitative analysis of cilia orientation (Fig. 2A-C left) showed a strong peak around 90°, with approximately 70% of WT cilia aligned toward the pia. In contrast, *reeler* outer layer neurons showed disrupted cilia orientation, with no predominant alignment toward the pial surface (Fig. 2A-B right). The corresponding histogram of cilia orientation (Fig. 2C right) revealed a more dispersed distribution of cilia angles, lacking the distinct peak observed in WT mice. Fitting the data with periodic normal distribution functions indicated that while WT cilia orientation followed a unimodal distribution centered around 90°, while the *reeler* data better fit a uniform distribution, indicative of randomized cilia orientation. Color-coded spatial maps (Fig. 2D) further supported this observation: WT samples showed similarly oriented cilia, while *reeler* samples exhibited a more heterogeneous and disorganized orientation pattern throughout the superficial layer.

However, *Reeler* is known to exhibit “outside-in” or inverted cortical lamination and the outer layer of *reeler* mostly contains early-born neurons, while its inner layer has late-born neurons

(D'Arcangelo et al., 1995; Ogawa et al., 1995), although the layer-specific boundary of *reeler* is not as sharp as WT (Hoffarth et al., 1995). To clearly distinguish early-born from late-born neurons, we used a Ctip2 antibody and a Satb2 antibody to label early- and late-born neurons, respectively. We also analyzed the apical-basal orientation of *reeler* neocortical neurons by examining cilia's apical location and axon's basal location at P10 and P30. An ankyrin G antibody was used to label the axon initial segment (AIS). At P10, both *reeler* early- and late-born neurons displayed disrupted cilia orientation, irregular apical localization, and disorganized axon initial segments (Fig. 3A-B). Cilia and AIS did not consistently align opposite to each other relative to nuclei either (Fig 3A-B). However, at P30, late-born *reeler* neurons manifested a remarkable improvement in cilia apical localization, orientation preference as well as relative separation between cilia and axon (Fig. 3D). In contrast, the improvement in early-born *reeler* neurons was much weaker: their cilia still lack a major orientation or localization preference, and the relative position from cilia to axon remains irregular (Fig. 3C). This suggests that early- and late-born neurons respond differentially to Reelin deficiency. Late-born neurons are more resistant to the impairments, because they undergo postnatal correction in apical-basal neuronal orientation.

To validate progressive correction in neuronal orientation in *reeler* late-born neurons, we measured cilia orientation of late-born neurons in the inner neocortex at P5, P10, P14, and P30 and analyzed cilia directionality and cilia localization (Fig. 4). At P5, cilia orientation was broadly distributed, with no dominant directional preference, suggesting early postnatal disorganization (Fig. 4Ai-iii). The histogram showed a minor peak oriented toward to the ventricular zone, and a flat distribution, largely indicating randomized cilia orientation (Fig. 4A-iv). At the same time, cilia were evenly distributed to 4 quadrants (Fig 4A-v). From P10 to P14, the angular distribution began to shift, with more cilia aligning between 60° and 120°, corresponding to orientation generally toward the pial surface. However, substantial variability remained, and the distribution lacked the sharp unimodal peak

typically observed in WT mice. By P30, cilia orientation became more focused, with a clearer peak near 90°, suggesting dominant alignment toward the pia, though some cilia still deviated from this axis. Simultaneously, cilia became increasingly enriched to the apical quadrant (Fig. 4B-D). These findings suggest that while cilia orientation remains incompletely aligned, directional organization of primary cilia of *reeler* late-born neurons emerges over time due to postnatal correction.

In contrast, primary cilia of reeler early-born neocortical neurons, marked by CTIP2 (Fig. 5C&F), maintain irregular orientation and random apical location at both P5 and P30, indicating that *reeler* early-born neurons do not undergo a postnatal correction in cilia orientation and apical-basal orientation from P5 to P30 (Fig. 5A-H). A diagram in Fig 5I summarizes the difference at P30: in WT superficial and deep layers, the cilia and centriole of both early- and late-born pyramidal neurons are localized to the base of the apical dendrites, with cilia predominantly oriented toward the pia. However, atypical pyramidal neurons in the deep layers exhibit irregular cilia orientation and random somal localization. In *reeler*, cilia of early-born neurons do not consistently align toward the pia or localize to the base of the apical dendrites. In contrast, the cilia of most late-born neurons at P30 are localized at the base of the apical dendrites and primarily oriented toward the pia. However, a portion of neuronal cilia still exhibit no directionality and lack apical localization.

Reelin Deficiency Partially Impairs the Apical Localization and Directional Orientation of Primary Cilia in CA1 Principal Neurons.

To examine how Reelin modulates ciliation pattern in the hippocampal CA1 region during postnatal development, we analyzed cilia orientation in *reeler* CA1 region at P10, P14, and P30. In the CA1 stratum pyramidale (SP) of WTs, primary cilia exhibit one major orientation toward the pia and one weak orientation toward the opposite direction (Fig. 6A, C and E), in line with our previous report (Yang et al., 2025). In contrast, *Reeler* CA1 neurons were not nicely layered, but roughly “top” and

“bottom” sublayers still distinguishable (B and D). In the top layer, cilia consistently exhibited a strong directional bias across ages from P10 - P30, with a predominant orientation centered around 270°, suggesting a preferred orientation toward pia (Figure 6F-H, left panels). In the bottom layer, cilia displayed a bimodal orientation pattern and subject to changes with age. At P10, the distribution was more diffuse, with lower and broader peaks at 97.8° and 274.1°, and ~41% and 59% of cilia in each orientation (Figure 6F, right panel). At P14, the peaks were present but broader, occurring at 96.7° and 275.2°, with ~45% and 55% of cilia oriented towards each direction, respectively (Figure 6G, right panel). At P30, two sharp and opposing peaks were observed at approximately 94.5° and 273.1°, with nearly equal proportions of cilia oriented in each direction (~49% and 51%, respectively) (Figure 6H, right panel).

Regarding cilia subcellular localization in CA1, cilia of WT CA1 principal neurons were predominantly localized to the apical dendrites (Table 1). In contrast, *reeler CA1* cilia initially were not predominantly localized to the apical quadrant at P10, and a large portion of cilia were also distributed to other quadrants (Fig. 6J). However, cilia localization underwent a postnatal re-alignment in the absence of Reelin, and cilia became preferably distributed near the base of apical dendrites at P30 (Fig. 6K). Together, these postnatal rectifications indicate that Reelin deficiency alters but does not completely disrupt cilia directional orientation and apical localization. This progressive changes in *reeler* from P10 to P30 suggest a somal re-positioning from the bottom to top during postnatal development, which recapitulates the backward movement of WT CA1 neurons observed from P7 to P14 (Yang et al., 2025).

Loss of Reelin strongly Alters the Orientation and Apical Localization of Cilia in Evolutionarily Conserved Cortical Regions

The piriform cortex, a major part of the olfactory cortex, is 3-layered paleocortex. The piriform cortex is also formed by an inside-out pattern (Martin-Lopez et al., 2019), but a more conserved cortical structure than the CA1 and neocortex (Klingler, 2017). We examined cilia orientation and subcellular localization in Layer II and III of the WT piriform cortex at P30 (Figure 7A). In Layer II, which is a compact lamina, neuronal primary cilia exhibit two major opposite directions (Fig 7B), while in Layer III which is sparsely layered, cilia have one major direction, predominately oriented toward the pial surface (Fig. 7C). Consistently, most of cilia (or centrioles) are localized near the base of apical dendrite (the apical quadrant) (Fig 7D). The loss of Reelin disrupts proper neuronal placement, laminated structures, and apical-basal neuron orientation in the piriform cortex (Figure 7E). We also found that primary cilia in the *reeler* piriform cortex no longer exhibit preferred orientation toward the pia and display irregular orientation (Figure 7F). Consistently, cilia base or centrioles were no longer localized to the base of apical dendrites, and they became randomly distributed in the soma (Figure 7G). These data indicate that reelin deficiency disrupts the directional orientation and subcellular localization of neuronal primary cilia in the piriform cortex. We also examined ciliation pattern in DG and CA3, which are also conserved cortical structures (Blackstad et al., 2022; Krubitzer and Seelke, 2012), compared to the CA1 and neocortex. Similarly, Reelin deficiency disrupts the lamination of principal neurons and perturbs the cilia orientation in the DG and the hippocampal CA3 region of P30 (Fig. S4). Together, Reelin strongly impairs the cilia orientation and apical localization of principal neurons in evolutionary low or conserved laminated regions, including piriform cortex, DG and CA3. Apparently, these conserved regions lack postnatal re-alignment in apical basal orientation in the absence of Reelin.

Primary Cilia of Excitatory Neurons in the Amygdala Exhibit Irregular Orientation and Subcellular Localization, Independent of Reelin.

To investigate whether Reelin influences cilia orientation in the amygdala, a non-laminated brain region (LeDoux, 2007), we analyzed the angular distribution of neuronal primary cilia in WT and *reeler* mice at P30 (Fig. S2A-B). Cilia orientation histograms and frequency distributions revealed that cilia in both groups exhibited broadly dispersed orientations across the full 360° range. No preferential alignment or consistent directional clustering was observed in either genotype (Fig. S2C&E). The degree of variability appeared similar in both WT and *reeler,* suggesting random orientation of primary cilia. Consistently, their cilia is relatively equally distributed to 4 quadrants of the soma, without a preference to the apical (Fig. S2D&F). These findings indicate that, unlike in laminated cortical regions, the amygdala displays inherently random cilia orientation, and this pattern is not altered by the loss of Reelin. Therefore, Reelin does not appear to regulate cilia orientation and subcellular localization in the amygdala and other non-laminated regions analyzed (Table 1).

Primary Cilia of Principal Neurons in the *Reeler* Cerebral Cortex Continue to Elongate after P14, When WT Cilia Stabilize.

Next, to examine if Reelin influences cilia morphology, we measured primary cilia length across different brain regions in WT and *reeler* mice. We performed immunofluorescence staining using AC3 antibody to specifically mark neuronal primary cilia (Bishop et al., 2007; Chen et al., 2016; Zhou et al., 2019) and Arl13b antibody to label astrocytic primary cilia (Sterpka and Chen, 2018; Sterpka et al., 2020). We analyzed cilia in WT and *reeler* mice at P14 and P30 - first focusing on laminated brain structures including the hippocampal CA1, CA3, DG, superficial and deep layers of the neocortex, piriform cortex, and entorhinal cortex.

In the hippocampal CA1 region, representative images (Fig. 8A, left) show visibly longer primary cilia in *reelers* compared to WTs. Quantitative analysis of cilia length, shown in the corresponding bar graph (Fig. 8A, right), confirmed a significant increase in cilia length in *reeler* mice.

This trend of elongated cilia was consistently observed in all other laminated regions analyzed, including CA3, DG, superficial neocortex, deep neocortex, piriform cortex, and entorhinal cortex (Fig. 8B-E, Table 2). At P14, cilia lengths in *reeler* mice were relatively comparable to those in WT controls across all regions, with minor differences detected (Fig. 8B-E, P14 groups). Additionally, WT mice exhibited stable cilia lengths between P14 and P30, indicating that cilia morphology remains relatively unchanged after P14, consistent with previous report (Yang et al., 2025). In contrast, *reeler* mice showed a pronounced and progressive elongation of primary cilia from P14 to P30 in all examined laminated brain regions. This age-dependent divergence suggests that Reelin is essential for constraining cilia growth during postnatal cortical development. Together, these findings demonstrate that Reelin helps maintain appropriate cilia length in the laminated cerebral cortex during postnatal development, and that its absence results in age-progressive cilia elongation likely associated with impaired lamination, although direct signaling effect from loss of Reelin cannot be excluded.

Loss of Reelin does not Affect the Cilia Length of Excitatory Neurons in Non-Laminated brain Regions, Interneurons or Astrocytes.

To determine whether Reelin influences primary cilia morphology in non-laminated brain regions, we measured cilia length in several such areas in WT and *reeler* mice at P30. These regions included the thalamus, striatum, hypothalamus, and amygdala. In the thalamus (Fig. S5A), immunofluorescence images (right panels) show similar cilia morphology between WT and *reeler* mice, and the corresponding bar graph (left panel) confirms no significant difference in cilia length. Likewise, in the striatum (Fig. S5B), hypothalamus (Fig. S5C), and amygdala (Fig. S5D), representative images on the right and quantitative analyses on the left consistently show no differences in cilia length between genotypes. These findings indicate that Reelin does not affect cilia length in non-laminated regions of

the brain. Statistical analysis using Student's *t*-test confirmed that all comparisons were not significant, indicating that the influence of Reelin on cilia morphology may be specific to laminated structures.

To determine whether Reelin affects cilia morphology in interneurons, we measured cilia length in WT and *reeler* mice at P30 using AC3 immunostaining in combination with interneuron-specific markers GAD65 (Kajita and Mushiake, 2021). In the CA1 region of the hippocampus, there was no significant difference in interneuron cilia length between genotypes (Figure S6A). Similarly, in both the deep and superficial layers of the neocortex, cilia length in interneurons did not differ between WT and *reeler* mice (Figure S6B-C). These findings demonstrate that Reelin does not influence primary cilia morphology in interneurons.

To determine whether Reelin affects cilia length in astrocytes, we measured cilia length in WT and *reeler* mice at P30 using Arl13b immunostaining with astrocyte-specific marker GFAP (Sterpka and Chen, 2018). In the CA1 region of the hippocampus, there was no significant difference in cilia length between genotypes (Figure S6D). Similarly, in both the deep and superficial layers of the neocortex, astrocytic cilia length did not differ between WT and *reeler* mice (Figure S6E-F). These findings indicate that Reelin does not affect primary cilia morphology in astrocytes.

Discussion

We have previously reported that principal neurons in inside-out laminated brain regions, especially late-born principal neurons, undergo a slow reverse movement for somal repositioning (Yang et al., 2025). Because of this, the primary cilia of principal neurons in inside-out laminated regions predominately orient toward the pial surface. This study addressed the question of what factor(s) control this unique cilia directionality. Here we present data showing that the primary cilia of principal neurons throughout

inside-out laminated regions, including the hippocampal CA1, piriform cortex and neocortex, are positioned to the base of the apical dendrite and aligned on the nuclear side opposite to the axon initial segment (Fig. 1 and S1-3, Table 1). In contrast, the primary cilia of interneurons, astrocytes, atypical pyramidal neurons in the deep neocortex, excitatory neurons in the amygdala and other non-laminated brain regions are irregularly positioned in the soma or around the nuclei and cilia lack directional orientation (Table 1). Because Reelin is a key determinator that influences neuronal placement and cortical lamination in the mammalian cerebral cortex (Jossin, 2020), we examined if Reelin affects the cilia directionality and cilia apical localization present in principal neurons. We employed *reeler* in our cilia orientation, localization and morphological analyses. *Reeler* is a well-characterized Reelin-deficient mouse strain, which manifests ectopic neuronal placement, “outside-in” cortical lamination or loss of layer-specific boundaries, and misorientation of apical-basal polarity, along with numerous other cellular and behavioral defects (Curran et al., 1995; D'Arcangelo et al., 1995; Falconer, 1951; Ogawa et al., 1995).

We discovered that the primary cilia of *reeler* early-born neurons in the neocortex, and principal neurons in evolutionarily conserved regions (DG and piriform cortex) do not display directional orientation, nor do their cilia localize to the base of the apical dendrite. In contrast, Reelin deficiency does not drastically disrupt the directional cilia orientation or their apical dendrite localization in late-born neurons in the neocortex and hippocampal CA1 region. This is because most *reeler* late-born neurons are initially misplaced in terms of apical-basal orientation and do not manifest cilia directional orientation and apical localization at early postnatal age. However, a large fraction can gradually rectify cilia orientation and apical localization, along with corrected apical-basal orientation, during late postnatal development. In addition, the primary cilia in principal neurons throughout the *reeler* cerebral cortex become longer than those of WT with postnatal age. In contrast, the length of primary cilia in

interneurons, astrocytes, or excitatory neurons in non-laminated brain regions are independent of Reelin signaling. The elongation of cilia length in *reeler* is in line with the alteration and rectification in cilia orientation and localization, all of which occurs in principal neurons in the cerebral cortex. Together, Reelin governs the directional orientation, intracellular localization, and length of primary cilia in principal neurons in the cerebral cortex.

Primary Cilia Represent an Important Apical Unit of Pyramidal Neurons in the Cerebral Cortex.

This study highlights primary cilia as an apical structure of principal neurons in the cerebral cortex. It seems evident how Reelin controls the subcellular localization of cilia in principal neurons. Reelin signaling plays a critical role in determining the subcellular localization of the centrosome in principal neurons in the cerebral cortex. As neurons complete their radial migration, Reelin, through activation of its receptors ApoER2 and VLDLR and subsequent downstream signaling, directs soma translocation and the positioning of the centrosome near the base of the apical dendrite (Chai and Frotscher, 2016; Cooper, 2008; Jossin, 2020; Trommsdorff et al., 1999). Reelin guidance on neuronal migration and the apical localization of the centrosome are essential for establishing primary cilia as an apical component of principal neurons in the cerebral cortex.

It is well-recognized that primary cilia regulate embryonic neurodevelopment through mediating signaling pathways, such as Sonic hedgehog (Bangs and Anderson, 2017) and Wnt signaling (Niehrs et al., 2025; Vuong and Mlodzik, 2023), to regulate cell fate specification, dorsal-ventral neural tube patterning, and neurogenesis (Das and Storey, 2014; Jang et al., 2016; Su et al., 2012; Yanardag and Pugacheva, 2021). Nevertheless, the roles of primary cilia in the postnatal brain remain largely unexplored. We show that the primary cilia of principal neurons in the cerebral cortex are localized near the base of the apical dendrite and predominantly orient toward the pial surface. This pattern is the most

prominent in late-born neurons in the neocortex and hippocampal CA1 region, somewhat mimicked by principal neurons in the piriform cortex, less pronounced in early born neocortical neurons and DG neurons and not present in atypical pyramidal neurons in the deep neocortex, excitatory neurons in non-laminated brain regions, or interneurons (Figure 1 & S1-3, Table 1). This suggests that the pattern is stronger among principal neurons which are born in the late developmental stage or appear later during cortical evolution.

Of relevance, we observed marked regional differences of *reeler* on cilia orientation and subcellular localization, which reflects the distinct impacts of Reelin on various cortical regions. In the DG and piriform cortex, loss of Reelin drastically disrupts layered structures, the primary cilia of principle neurons do not exhibit cilia directional orientation and apical dendrite localization (Fig. S4, Table 1). This phenomenon was similarly observed among early-born neurons in the neocortex (Fig. 5). However, late-born neurons in the neocortex (Fig. 3-4) and hippocampal CA1 regions (Fig. 6) manifest resistance to Reelin deficiency. Consistently, the primary cilia of late-born neurons in the CA1 and neocortex are postnatally corrected to be preferably localized to the apical dendrite and mainly orient toward the pia (Fig. 4&6). Thus, the apical dendrite localization of primary cilia and their directional orientation are linked to the apical-basal neuronal orientation and proper layering.

What is the biological significance of cilia localization near the base of the apical dendrite of principal neurons, which is clearly distant from the AIS on the opposite side of the nucleus (Fig. 1, Table 1)? Interestingly, this phenomenon is not observed in other cell types or excitatory neurons in nucleated regions (Fig. S2-3, Table 1). Thus, the relative distance and localization of cilia, as signal input, and axon, as electrical output, is sharply defined in principal neurons in the cerebral cortex, but is irregular among other cells or non-laminated brain regions. Primary cilia function as signaling hubs that receive and integrate extracellular cues into the soma (Valente et al., 2014). A variety of receptors including

GPCRs and downstream signaling molecules have been identified in neuronal primary cilia (Mukhopadhyay and Rohatgi, 2014; Pal and Mukhopadhyay, 2015; Tschaikner et al., 2020; Wang and Ogden, 2025). A well-defined cilia-in-apical and axon-at-basal locations may aid in spatial coordination of signaling along the apical-basal axis of principal neurons in the cerebral cortex. Additionally, this structural setting may avoid too strong influence of ciliary input on AIS output. Conversely, an irregular cilia-AIS localization present in neurons in non-laminated brain regions does not confer this advantage. Given the primary cilia of principal neurons is an apical input component, it is tempting to speculate that disruption of cilia structure or key cilia signaling may lead to perturbation in apical function. Further, primary cilia may not only serve as sensory antenna but also may contribute to the refinement of the apical polarity of principal neurons, particularly among late-born neurons in the cerebral cortex.

Reelin Deficiency Promotes Cilia Elongation in Principal Neurons likely through Disrupted Cortical Lamination.

We have shown that loss of Reelin in *reeler* leads to postnatally elongated cilia in principal neurons throughout the cerebral cortex, including DG, hippocampal CA1 and CA3, neocortex, piriform cortex, and entorhinal cortex (Fig. 8 and Table 2). We have previously reported that the primary cilia of principal neurons in the cerebral cortex of C57Bl6 WT mice emanate during the postnatal stage with exact timing depending on brain regions, for example, around P8-P14 in the hippocampal CA1 (Yang et al., 2025). Cilia elongation in the cerebral cortex largely completes ~ P14 and cilia length does not change much afterwards (Fig. 8 and Table 2). In this study, we found that the cilia length in the WT and *reeler* cerebral cortex is not markedly different at P14 (Figure 8, Table 2), but the primary cilia of *reeler* principal neurons throughout the cerebral cortex continue to elongate after P14. The differences in cilia length between *reeler* and WT thereby become much stronger at P30 than P14 (Table 2).

Since Reelin regulates key processes such as neuronal migration, polarity, and cytoskeletal dynamics (Frotscher et al., 2009; Jossin, 2020; Matsuki et al., 2010), its absence leads to impaired neuronal migration. As a result, layering of neurons in the adult cortex is approximately inverted (Rugarli and Ballabio, 1995). Reelin also functions as a stop signal for neuronal migration during development (Frotscher et al., 2009). This suggests that in *reeler* mice, the observed elongation of primary cilia likely represents a secondary consequence of broader neuronal disorganization resulting from impaired lamination. We postulate that the absence of this stop signal disrupts normal developmental cues, leading to dysregulated cilia elongation. Alternatively, due to unsuccessful neuronal placement, *reeler* neurons continue to adjust positioning, while longer primary cilia may contribute to re-positioning process.

A clear distinction in cilia length caused by Reelin deficiency was identified between laminated cortical structures, such as the hippocampal CA1, piriform cortex, and neocortex etc, and non-laminated regions such as amygdala, thalamus, hypothalamus etc. Laminated regions are strongly affected by Reelin for neuronal placement and apical-basal neuronal orientation, most principal neurons there also show directional cilia orientation, whereas neurons in nucleated regions do not. This supports the interpretation that the observed cilia elongation specifically in principal neurons in the cerebral cortex is closely linked to the disruption of laminar architecture. Concurrent with cilia prolongation after P14, cilia orientation and apical localization in late-born neurons continue to rectify over the course of postnatal development (Fig. 2-4). As primary cilia are involved in refining neuronal positioning (Yang et al., 2025), the cilia elongation after P14 is more likely a compensatory growth to adjust somal positioning. In line with this interpretation, no differences on cilia length were detected in interneurons and astrocytes throughout the WT and *reeler* brains. Likewise, this is because these cell types are not laminated in the brain.

Distinct Cilia Phenotypes of Early- and Late-born Neurons in the Postnatal Brain in the Absence of Reelin

In the mammalian cerebral cortex, early- and late-born neurons differ markedly in their birthtime, laminar destiny, gene expression pattern, connectivity, and brain functions (Barbas, 2015; Cooper, 2008; Kohwi and Doe, 2013; Marin and Rubenstein, 2003). Early-born neurons are generated first (E10 - E13 in WT mice) and settle in deep Layers (Cooper, 2008; Shepherd and Rowe, 2017). They tend to execute basic cortical functions such as sensory and motor processing. In contrast, late-born neurons are produced around E14 - E18 and reside in superficial Layers (Cooper, 2008). Late-born neurons are more engaged in higher brain function such as working memory and complex cognition. We have previously reported that late-born neurons in the CA1 and neocortex are subject to a reverse post-migratory somal re-positioning, while early-born neurons may not (Yang et al., 2025). Even if some early-born neurons move backwards slightly depending on their specific location, they may passively follow the backward squeezing of late-born neurons. Because of this difference, late-born neurons manifest cilia orientation clearly toward the pial surface, while the cilia orientation of early-born neurons in deep layers vary greatly, albeit still pointing in the pia direction (Yang et al., 2025) (Fig. 1G).

Reelin is important not only for guiding neuronal placement but also for helping establish the apical-basal orientation of principal neurons in the cerebral cortex (Kupferman et al., 2014; Matsuki et al., 2010). Intriguingly, loss of Reelin affects the placement of early-born and late-born neurons differentially. Early-born *reeler* neurons exhibit severely disrupted apical-basal polarity, aberrant axon orientation (ref) and abnormal cell shape (ref). In contrast, late-born *reeler* neurons partially retain apical-basal orientation and exhibit postnatal correction (ref). Likewise, we have identified distinct phenotypes in cilia orientation and apical localization among early-born and late-born *reeler* neocortical neurons. Reelin deficiency affects the cilia orientation and localization of early-born neurons more

severely than late-born neurons. Late-born neurons exhibit postnatal correction in cilia orientation and localization, while early-born neurons do not (Fig. 2-5). Correspondingly, in the hippocampal CA1 region where most neurons are late-born neurons, *reeler* laminar structure is partially maintained or corrected to some degree postnatally, so does cilia apical localization (Fig. 6).

We interpret these differences in the context of cortical evolution in relation to postnatal neurodevelopment, although alternative explanations cannot be excluded. We postulate that late-born neurons that emerge at later developmental stages may acquire new capacities, potentially enabling them to construct intricate neural networks and support higher-order brain functions. The reversal somal repositioning that occurs postnatally may be one of new capacities that late-born neurons have acquired. Besides fine-tune positioning to support gradual neuronal maturation and orderly construction of neural connectivity, the reverse somal repositioning may enhance the directional cilia orientation and apical-basal polarity of pyramidal neurons, allowing individual late-born neurons to sort and process information more efficiently. In addition, the reverse movement may likely confer late-born neurons the ability to resist lamina disturbance in the absence of Reelin or postnatally correct neuronal misorientation. However, this speculation warrants further investigation and validation.

Irregular Orientation and Subcellular Localization of Primary Cilia in Atypical Pyramidal Neurons in the Deep Neocortex and Excitatory Neurons in Non-laminated Brain Regions.

All principal neurons in the cerebral cortex, except for atypical pyramidal neurons in the deep neocortex, have cilia localization near the base of apical dendrites (Table 1, Fig. S2-3). Why? We reason that the birthtime of these atypical pyramidal neurons may limit their exposure to Reelin. Cajal-Retzius cells begin secreting Reelin around embryonic day 10.5 (E10.5) (Hevner et al., 2003; Soriano and Del Rio, 2005). The levels and gradient strength continue to increase over time, peaking as the cortical plate thickens (Elorriaga et al., 2023). Layer VI neurons, among the earliest-born cortical neurons, migrate

and settle in the cortical plate before the full establishment of Reelin gradients near the marginal zone (or Layer I) (Causeret et al., 2021). As a result, these early-born neurons may experience lower levels of Reelin or rely less on Reelin-dependent cues for migration termination and apical-basal orientation. This weak exposure to Reelin during their migratory window may contribute to “inverted or atypical” neuronal orientation and cell shape (Steger et al., 2018; Steger et al., 2013), and irregular cilia localization and orientation in the deep neocortex (Table 1). We also examined the cilia orientation and subcellular localization of excitatory neurons in the amygdala, which is not a laminated structure, and found the ciliation pattern resemble that of atypical pyramidal neurons in the deep neocortex (Fig S2 and Table 1) (Yang et al., 2025). Furthermore, interneurons, astrocytes, and excitatory neurons in other non-laminated brain regions such as thalamus and hypothalamus also exhibit irregular cilia orientation and subcellular localization (Table 1). All these cells or brain regions are not laminated organized or strongly affected by Reelin for neuronal placement. Together, these data substantiate the interpretation that Reelin is a crucial factor that control primary cilia orientation and subcellular localization of principal neurons. Thus, the cilia directionality of principal neurons is highly correlated with cortical lamination.

How does Reelin Affect Directional Cilia Orientation of Principal Neurons?

How does Reelin influences the apical localization and directional orientation of primary cilia in principal neurons in inside-out laminated regions? Thus far, we have no evidence that Reelin directly interacts with primary cilia during postnatal development. However, this does not exclude the possibility that Reelin downstream signal proteins crosstalk with cilia or ciliary downstream proteins to modulate cytoskeleton remodeling. Results from this research, along with our previous study (Yang et al., 2025), support a model in which Reelin guides embryonic neuronal migration toward the pial surface and termination of soma translocation, which leads to accumulation of late-born neurons in the outer layers

beneath the marginal zone. During postnatal development, due to neuronal growth and crowding, late-born neurons undergo a slow reverse soma repositioning toward sparse inner regions. Early-born neurons in the deep layers, depending on locations, may not actively reverse but may be passively squeezed by late-born neurons to reverse. This results in directional cilia orientation most prominently in late-born neurons, less in early-born neurons, and absent in atypical pyramidal neurons in the deep cortex. Excitatory neurons in non-laminated brain regions are not strongly affected by Reelin for layering; therefore, they do not show preferred cilia orientation and apical localization. Thus, it is the neuronal aggregation in the outer layers induced by Reelin that drives reverse soma repositioning. This model also predicts that over the course of cortical evolution, if more late-born neurons are generated to accumulate in outer cortical layers in a mammalian species and in mutant mouse strains, its reversed re-positioning would become stronger, and a higher percentage of neurons would gain directional cilia orientation.

References:

Alexander, A., J. Herz, and L. Calvier. 2023. Reelin through the years: From brain development to inflammation. *Cell Rep*. 42:112669.

Bangs, F., and K.V. Anderson. 2017. Primary Cilia and Mammalian Hedgehog Signaling. *Cold Spring Harb Perspect Biol*. 9.

Barbas, H. 2015. General cortical and special prefrontal connections: principles from structure to function. *Annu Rev Neurosci*. 38:269-289.

Bishop, G.A., N.F. Berbari, J. Lewis, and K. Mykytyn. 2007. Type III adenylyl cyclase localizes to primary cilia throughout the adult mouse brain. *J Comp Neurol*. 505:562-571.

Blackstad, J.S., K.K. Osen, and T.B. Leergaard. 2022. The fibro- and cyto-architecture demarcating the border between the dentate gyrus and CA3 in sheep (Ovis aries) and domestic pig (Sus scrofa domesticus). *Hippocampus*. 32:639-659.

Breunig, J.J., M.R. Sarkisian, J.I. Arellano, Y.M. Morozov, A.E. Ayoub, S. Sojitra, B. Wang, R.A. Flavell, P. Rakic, and T. Town. 2008. Primary cilia regulate hippocampal neurogenesis by mediating sonic hedgehog signaling. *Proc Natl Acad Sci U S A*. 105:13127-13132.

Causeret, F., M.X. Moreau, A. Pierani, and O. Blanquie. 2021. The multiple facets of Cajal-Retzius neurons. *Development*. 148.

Chai, X., and M. Frotscher. 2016. How does Reelin signaling regulate the neuronal cytoskeleton during migration? *Neurogenesis (Austin)*. 3:e1242455.
Chen, X., J. Luo, Y. Leng, Y. Yang, L.S. Zweifel, R.D. Palmiter, and D.R. Storm. 2016. Ablation of type III adenylyl cyclase in mice causes reduced neuronal activity, altered sleep pattern, and depression-like phenotypes. *Biol Psychiatry*. 80:836-848.
Cooper, J.A. 2008. A mechanism for inside-out lamination in the neocortex. *Trends Neurosci*. 31:113-119.
Curran, T., G. D'Arcangelo, and A. Goffinet. 1995. Reeler gene discrepancies. *Nat Genet*. 11:12-13.
D'Arcangelo, G., G.G. Miao, S.C. Chen, H.D. Soares, J.I. Morgan, and T. Curran. 1995. A protein related to extracellular matrix proteins deleted in the mouse mutant reeler. *Nature*. 374:719-723.
Das, R.M., and K.G. Storey. 2014. Apical abscission alters cell polarity and dismantles the primary cilium during neurogenesis. *Science*. 343:200-204.
Elorriaga, V., A. Pierani, and F. Causeret. 2023. Cajal-retzius cells: Recent advances in identity and function. *Curr Opin Neurobiol*. 79:102686.
Falconer, D.S. 1951. Two new mutants, 'trembler' and 'reeler', with neurological actions in the house mouse (Mus musculus L.). *J Genet*. 50:192-201.
Frotscher, M., X. Chai, H.H. Bock, C.A. Haas, E. Forster, and S. Zhao. 2009. Role of Reelin in the development and maintenance of cortical lamination. *J Neural Transm (Vienna)*. 116:1451-1455.
Green, J.A., and K. Mykytyn. 2014. Neuronal primary cilia: an underappreciated signaling and sensory organelle in the brain. *Neuropsychopharmacology*. 39:244-245.
Hasenpusch-Theil, K., and T. Theil. 2021. The multifaceted roles of primary cilia in the development of the cerebral cortex. *Front Cell Dev Biol*. 9:630161.
Hattori, M. 2025. Regulatory mechanism of Reelin activity: a platform for exploiting Reelin as a therapeutic agent. *Front Mol Neurosci*. 18:1546083.
Hevner, R.F., T. Neogi, C. Englund, R.A. Daza, and A. Fink. 2003. Cajal-Retzius cells in the mouse: transcription factors, neurotransmitters, and birthdays suggest a pallial origin. *Brain Res Dev Brain Res*. 141:39-53.
Ho, E.K., and T. Stearns. 2021. Hedgehog signaling and the primary cilium: implications for spatial and temporal constraints on signaling. *Development*. 148.
Hoffarth, R.M., J.G. Johnston, L.A. Krushel, and D. van der Kooy. 1995. The mouse mutation reeler causes increased adhesion within a subpopulation of early postmitotic cortical neurons. *J Neurosci*. 15:4838-4850.
Howell, B.W., R. Hawkes, P. Soriano, and J.A. Cooper. 1997. Neuronal position in the developing brain is regulated by mouse disabled-1. *Nature*. 389:733-737.
Ishii, K., K.I. Kubo, and K. Nakajima. 2016. Reelin and Neuropsychiatric Disorders. *Front Cell Neurosci*. 10:229.
Jang, J., Y. Wang, M.A. Lalli, E. Guzman, S.E. Godshalk, H. Zhou, and K.S. Kosik. 2016. Primary Cilium-Autophagy-Nrf2 (PAN) Axis Activation Commits Human Embryonic Stem Cells to a Neuroectoderm Fate. *Cell*. 165:410-420.
Joly-Amado, A., N. Kulkarni, and K.R. Nash. 2023. Reelin Signaling in Neurodevelopmental Disorders and Neurodegenerative Diseases. *Brain Sci*. 13.
Jossin, Y. 2020. Reelin Functions, Mechanisms of Action and Signaling Pathways During Brain Development and Maturation. *Biomolecules*. 10.

Kajita, Y., and H. Mushiake. 2021. Heterogeneous GAD65 expression in subtypes of GABAergic neurons across layers of the cerebral cortex and hippocampus. *Front Behav Neurosci*. 15:750869.
Katsuyama, Y., and M. Hattori. 2024. REELIN ameliorates Alzheimer's disease, but how? *Neurosci Res*. 208:8-14.
Klingler, E. 2017. Development and Organization of the Evolutionarily Conserved Three-Layered Olfactory Cortex. *eNeuro*. 4.
Kohwi, M., and C.Q. Doe. 2013. Temporal fate specification and neural progenitor competence during development. *Nat Rev Neurosci*. 14:823-838.
Krubitzer, L.A., and A.M. Seelke. 2012. Cortical evolution in mammals: the bane and beauty of phenotypic variability. *Proc Natl Acad Sci U S A*. 109 Suppl 1:10647-10654.
Kupferman, J.V., J. Basu, M.J. Russo, J. Guevarra, S.K. Cheung, and S.A. Siegelbaum. 2014. Reelin signaling specifies the molecular identity of the pyramidal neuron distal dendritic compartment. *Cell*. 158:1335-1347.
Landrieu, P., and A. Goffinet. 1981. Inverted pyramidal neurons and their axons in the neocortex of reeler mutant mice. *Cell Tissue Res*. 218:293-301.
LeDoux, J. 2007. The amygdala. *Curr Biol*. 17:R868-874.
Lee, J.E., and J.G. Gleeson. 2011. Cilia in the nervous system: linking cilia function and neurodevelopmental disorders. *Curr Opin Neurol*. 24:98-105.
Macarelli, V., E. Leventea, and F.T. Merkle. 2023. Regulation of the length of neuronal primary cilia and its potential effects on signalling. *Trends Cell Biol*. 33:979-990.
Marin, O., and J.L. Rubenstein. 2003. Cell migration in the forebrain. *Annu Rev Neurosci*. 26:441-483.
Martin-Lopez, E., K. Ishiguro, and C.A. Greer. 2019. The Laminar Organization of Piriform Cortex Follows a Selective Developmental and Migratory Program Established by Cell Lineage. *Cereb Cortex*. 29:1-16.
Matsuki, T., R.T. Matthews, J.A. Cooper, M.P. van der Brug, M.R. Cookson, J.A. Hardy, E.C. Olson, and B.W. Howell. 2010. Reelin and stk25 have opposing roles in neuronal polarization and dendritic Golgi deployment. *Cell*. 143:826-836.
Mukhopadhyay, S., and R. Rohatgi. 2014. G-protein-coupled receptors, Hedgehog signaling and primary cilia. *Semin Cell Dev Biol*. 33:63-72.
Niehrs, C., F. Da Silva, and C. Seidl. 2025. Cilia as Wnt signaling organelles. *Trends Cell Biol*. 35:24-32.
Ogawa, M., T. Miyata, K. Nakajima, K. Yagyu, M. Seike, K. Ikenaka, H. Yamamoto, and K. Mikoshiba. 1995. The reeler gene-associated antigen on Cajal-Retzius neurons is a crucial molecule for laminar organization of cortical neurons. *Neuron*. 14:899-912.
Pal, K., and S. Mukhopadhyay. 2015. Primary cilium and sonic hedgehog signaling during neural tube patterning: role of GPCRs and second messengers. *Dev Neurobiol*. 75:337-348.
Phua, S.C., S. Chiba, M. Suzuki, E. Su, E.C. Roberson, G.V. Pusapati, S. Schurmans, M. Setou, R. Rohatgi, J.F. Reiter, K. Ikegami, and T. Inoue. 2019. Dynamic remodeling of membrane composition drives cell cycle through primary cilia excision. *Cell*. 178:261.
Rice, D.S., and T. Curran. 2001. Role of the reelin signaling pathway in central nervous system development. *Annu Rev Neurosci*. 24:1005-1039.
Rugarli, E.I., and A. Ballabio. 1995. Reelin: a novel extracellular matrix protein involved in brain lamination. *Bioessays*. 17:832-834.

Sasai, N., and J. Briscoe. 2012. Primary cilia and graded Sonic Hedgehog signaling. *Wiley Interdiscip Rev Dev Biol*. 1:753-772.
Sheldon, M., D.S. Rice, G. D'Arcangelo, H. Yoneshima, K. Nakajima, K. Mikoshiba, B.W. Howell, J.A. Cooper, D. Goldowitz, and T. Curran. 1997. Scrambler and yotari disrupt the disabled gene and produce a reeler-like phenotype in mice. *Nature*. 389:730-733.
Shepherd, G.M., and T.B. Rowe. 2017. Neocortical Lamination: Insights from Neuron Types and Evolutionary Precursors. *Front Neuroanat*. 11:100.
Singla, V., and J.F. Reiter. 2006. The primary cilium as the cell's antenna: signaling at a sensory organelle. *Science*. 313:629-633.
Sipos, E., S. Komoly, and P. Acs. 2018. Quantitative Comparison of Primary Cilia Marker Expression and Length in the Mouse Brain. *J Mol Neurosci*. 64:397-409.
Soriano, E., and J.A. Del Rio. 2005. The cells of cajal-retzius: still a mystery one century after. *Neuron*. 46:389-394.
Steger, R., L. Blachorsky, Q. Yang, and J.C. Brumberg. 2018. Synaptic properties of layer VI inverted pyramidal cells in the rodent somatosensory cortex. *Somatosens Mot Res*. 35:33-44.
Steger, R.M., R.L. Ramos, R. Cao, Q. Yang, C.C. Chen, J. Dominici, and J.C. Brumberg. 2013. Physiology and morphology of inverted pyramidal neurons in the rodent neocortex. *Neuroscience*. 248:165-179.
Sterpka, A., and X. Chen. 2018. Neuronal and astrocytic primary cilia in the mature brain. *Pharmacol Res*. 137:114-121.
Sterpka, A., J. Yang, M. Strobel, Y. Zhou, C. Pauplis, and X. Chen. 2020. Diverged morphology changes of astrocytic and neuronal primary cilia under reactive insults. *Mol Brain*. 13:28.
Stranahan, A.M., J.R. Erion, and M. Wosiski-Kuhn. 2013. Reelin signaling in development, maintenance, and plasticity of neural networks. *Ageing Res Rev*. 12:815-822.
Su, C.Y., S.N. Bay, L.E. Mariani, M.J. Hillman, and T. Caspary. 2012. Temporal deletion of Arl13b reveals that a mispatterned neural tube corrects cell fate over time. *Development*. 139:4062-4071.
Trommsdorff, M., M. Gotthardt, T. Hiesberger, J. Shelton, W. Stockinger, J. Nimpf, R.E. Hammer, J.A. Richardson, and J. Herz. 1999. Reeler/Disabled-like disruption of neuronal migration in knockout mice lacking the VLDL receptor and ApoE receptor 2. *Cell*. 97:689-701.
Tschaikner, P., F. Enzler, O. Torres-Quesada, P. Aanstad, and E. Stefan. 2020. Hedgehog and Gpr161: Regulating cAMP Signaling in the Primary Cilium. *Cells*. 9.
Tu, H.Q., S. Li, Y.L. Xu, Y.C. Zhang, P.Y. Li, L.Y. Liang, G.P. Song, X.X. Jian, M. Wu, Z.Q. Song, T.T. Li, H.B. Hu, J.F. Yuan, X.L. Shen, J.N. Li, Q.Y. Han, K. Wang, T. Zhang, T. Zhou, A.L. Li, X.M. Zhang, and H.Y. Li. 2023. Rhythmic cilia changes support SCN neuron coherence in circadian clock. *Science*. 380:972-979.
Valente, E.M., R.O. Rosti, E. Gibbs, and J.G. Gleeson. 2014. Primary cilia in neurodevelopmental disorders. *Nat Rev Neurol*. 10:27-36.
Vuong, L.T., and M. Mlodzik. 2023. The complex relationship of Wnt-signaling pathways and cilia. *Curr Top Dev Biol*. 155:95-125.
Wang, C.E., and S.K. Ogden. 2025. G Protein-Coupled Receptor Signal Intersection at the Primary Cilium. *Bioessays*. 47:e70015.
Wilsch-Bräuninger, M., and W.B. Huttner. 2021. Primary cilia and centrosomes in neocortex development. *Front Neurosci*. 15:755867.

Yanardag, S., and E.N. Pugacheva. 2021. Primary Cilium Is Involved in Stem Cell Differentiation and Renewal through the Regulation of Multiple Signaling Pathways. *Cells*. 10.

Yang, J., S. Mirhosseiniardakani, L. Qiu, K. Bicja, A. Del Greco, K.J. Lin, M. Lyon, and X. Chen. 2025. Cilia directionality reveals a slow reverse movement of principal neurons for positioning and lamina refinement in the cerebral cortex. *Development*. 152.

Yoneshima, H., E. Nagata, M. Matsumoto, M. Yamada, K. Nakajima, T. Miyata, M. Ogawa, and K. Mikoshiba. 1997. A novel neurological mutant mouse, yotari, which exhibits reeler-like phenotype but expresses CR-50 antigen/reelin. *Neurosci Res*. 29:217-223.

Zhou, Y., L. Qiu, A. Sterpka, H. Wang, F. Chu, and X. Chen. 2019. Comparative Phosphoproteomic Profiling of Type III Adenylyl Cyclase Knockout and Control, Male, and Female Mice. *Front Cell Neurosci*. 13:34.

Table 1: Cilia Orientation and Intracellular Localization in Brain Regions of WT and *reeler* Mice

Brain Regions or Cell Types	WT (P30)			*Reeler* (P30)		
	Cilia Orientation	Lemina Cell Density	Cilia/Centriole Localization	Cilia Orientation	Lemina Cell Density	Cilia/Centriole Localization
DG	Irregular	Compact	Irregular	Random	Disorganized	Irregular
Dorsal CA1	Opposite, mainly toward the pia	Compact	base of apical dendrite	Opposite	Compact, Split SP	Mainly base of apical dendrite, Some irregular,
Ventral CA1	Opposite, mainly toward the pia	Compact	base of apical dendrite	Opposite	Compact, Split SP	Mainly base of apical dendrite, Some irregular
Neocortex (Late-born)	Oriented to the pia	Sparse	base of apical dendrite	mostly Oriented to the pia	Inverted, partially affected	Mostly, base of apical dendrite, Some irregular
Neocortex (Early-born)	Oriented to the pia	Sparse	Mostly at base of apical dendrite	Random	Inverted Disorganized	Irregular
Piriform Cortex (Layer II)	Opposite	Compact	base of apical dendrite	Random	Inverted Disorganized	Irregular
Piriform Cortex (Layer III)	Orient to the pia	Sparse	base of apical dendrite	Random	Inverted Disorganized	Irregular
Cingulate Cortex	Orient to the pia	Compact /Sparse	base of apical dendrite	Random	Inverted Disorganized	Irregular
CA1 Interneurons	Irregular	Not layered	Irregular	Irregular	Not layered	Irregular
Neocortex Interneurons	Irregular	Not layered	Irregular	Irregular	Not layered	Irregular
CA1 Astrocytes	Irregular	Not layered	Irregular	Irregular	Not layered	Irregular
Neocortex Astrocytes	Irregular	Not layered	Irregular	Irregular	Not layered	Irregular
Thalamus	Irregular	Not layered	Irregular	Irregular	Not layered	Irregular
Hypothalamus	Irregular	Not layered	Irregular	Irregular	Not layered	Irregular
Amygdala	Irregular	Not layered	Irregular	Irregular	Not layered	Irregular
Striatum	Irregular	Not layered	Irregular	Irregular	Not layered	Irregular

Table 2: Cilia Length in Various Brain Regions and Cell Types of WT and *reeler* Mice

Brain Region	Layering	P14		P30	
		WT (µm)	*reeler* (µm)	WT (µm)	*reeler* (µm)
CA1	Laminated	5.21 ± 0.36	5.86 ± 0.18 (*)	5.38 ± 0.33	8.62 ± 0.88 (***)
CA3	Laminated	5.13 ± 0.24	5.72 ± 0.14 (*)	5.32 ± 0.27	7.04 ± 0.22 (***)
DG	Laminated	2.82 ± 0.13	3.64 ± 0.16 (**)	2.90 ± 0.15	5.02 ± 0.20 (***)
Deep Neocortex	Laminated	4.31 ± 0.10	4.82 ± 0.20 (*)	4.49 ± 0.17	5.92 ± 0.10 (***)
Superficial Neocortex	Laminated	5.23 ± 0.11	5.71 ± 0.07 (**)	5.36 ± 0.07	6.88 ± 0.20 (***)
Piriform Cortex	Laminated	4.61 ± 0.25	5.12 ± 0.13 (*)	4.83 ± 0.09	6.02 ± 0.27 (**)
Entorhinal Cortex	Laminated	4.80 ± 0.27	5.33 ± 0.11 (*)	5.15 ± 0.14	6.01 ± 0.08 (***)
Thalamus	Non-laminated	ND	ND	5.53 ± 0.32	5.53 ± 0.34 (n.s.)
Hypothalamus	Non-laminated	ND	ND	5.48 ± 0.35	5.53 ± 0.33 (n.s.)
Amygdala	Non-laminated	ND	ND	5.28 ± 0.14	5.29 ± 0.16 (n.s.)
Striatum	Non-laminated	ND	ND	6.41 ± 1.02	6.43 ± 1.01 (n.s.)
Astrocyte CA1	Non-laminated	ND	ND	5.12 ± 0.01	5.14 ± 0.03 (n.s.)
Astrocyte deep cortex	Non-laminated	ND	ND	4.25 ± 0.14	4.34 ± 0.11 (n.s.)
Astrocyte Superficial Cortex	Non-laminated	ND	ND	4.51 ± 0.07	4.50 ± 0.06 (n.s.)
Interneuron CA1	Non-laminated	ND	ND	5.09 ± 0.11	5.13 ± 0.14 (n.s.)
Interneuron Deep Cortex	Non-laminated	ND	ND	5.13 ± 0.19	5.11 ± 0.10 (n.s.)
Interneuron Superficial Cortex	Non-laminated	ND	ND	5.16 ± 0.34	5.17 ± 0.31 (n.s.)

Figure Legends:

Figure 1. Primary cilia of neocortical principal neurons are predominantly localized near the base of apical dendrites and aligned opposite to the axon initial segment relative to the nuclei. (A-C) Representative images showing neuronal cilia orientation and cilia intracellular localization in the superficial neocortical layers. **(A)** Neurons in the superficial layers marked by a NeuN antibody. **(B)** Excitatory neurons marked by an Glutaminase II antibody. **(C)** (Left) A diagram showing how four quadrants (Apical, Basal, Lateral-left and Lateral-right) was defined in reference to the center of nucleus and the apical dendrite marked by a NeuN antibody. The position of cilia base in a quadrant was used to determine cilia intracellular localization. (Right) Cilia or centrioles of superficial principal neurons were mainly distributed to the apical quadrant. **(D-F)** Late-born neurons cilia orientation and localization relative to the axon initial segment. **(D)** Representative images showing cilia aligned opposite to the axon initial segment relative to the nuclei. **(E)** Cilia orientation histogram of late-born neurons. **(F)** Cilia and centrioles of late-born neurons were predominantly distributed to the apical quadrant. **(G-I)** Early-born neurons cilia orientation and intracellular localization. **(H)** Cilia orientation histogram of early-born neurons. The preference of cilia orientation in early-born neurons toward the pial surface was weaker than in late-born neurons. **(I)** Cilia and centrioles of early-born neurons were mostly distributed to the apical quadrant, while still a lot disperse to other quadrants. **E and H** were fitted with one or two periodic normal distribution density functions, combined with a uniform distribution.

Figure 2. Disrupted cilia orientation in the outer layer of the *reeler* neocortex. (A-B) Primary cilia in the outer layer of the WT and *reeler* neocortices. WT cilia were mostly localized to the apical dendrites and oriented to the pial surface, while *reeler* cilia irregularly distributed to the soma and lacked preferred orientation. **(C)** Histograms of cilia orientations in the outer layers of the reeler neocortex. ~70% WT

neocortical cilia oriented toward the pia (peak at ~90°). In contrast, *reeler* neuronal cilia did not orient toward the pial surface. Data were fitted with one or two periodic normal distribution density functions, combined with a uniform distribution. **(D)** Orientation map in the outer layers visualizing cilia orientation across the sampled fields, color-coded by angle (degrees). Data were pooled from multiple sections out of 3-5 *reeler* and WT brains.

Figure 3. *Reeler* late-born neurons exhibit a much stronger postnatal rectification in apical-basal orientation than early-born neurons. *Reeler* early-born neurons **(A)** and late-born neurons **(B)** at P10; early-born neurons **(C)** and late-born neurons **(D)** at P30. Primary cilia, AIS, early- and late-born neurons were labeled by AC3, Ankyrin G, CTIP2 or Satb2 antibodies, respectively. At P10, misoriented cilia and axon present in both early- and late born neurons. At P30, most late-born neurons' cilia localized to the apical quadrant and axons to the basal quadrant, while early-born neuron's cilia were randomly distributed to four quadrants.

Figure 4. *reeler* late-born neocortical neurons are subject to gradual correction in cilia orientation and cilia apical localization during postnatal development. (A-D) *reeler* late-born neurons at different postnatal ages: P5 (**A**), P10 (**B**), P14 (**C**) and P30 (**D**). (**i**) Images of late-born neurons and primary cilia marked by Satb2 and AC3 antibodies, respectively. (**ii**) Images of late-born neurons and cilia marked by NeuN and AC3 antibodies, respectively. NeuN staining can display the apical dendrites. (**iii**) Representative images of individual neurons with apical dendrites and cilia. (**iv**) Cilia orientation of late-born neurons at different ages. Histograms of cilia orientation with fitting curves of periodic normal distribution density function. (**v**) Cilia intracellular localization in four quadrants at different ages. At P5

and P10, cilia in late-born *reeler* neurons had broad angular distributions with partial directional bias. By P30, cilia exhibit a more defined orientation toward the pia, in line with gradual changes in apical localization with age.

Figure 5. *reeler* early-born neocortical neurons do not exhibit postnatal correction in cilia orientation and apical localization from P5 to P30. (A-B) cilia of *reeler* early-born neurons at P5 **(A)** and P30 **(B)**. Cilia lack preferred orientation and preferred apical localization. Early-born *reeler* neurons at P5 **(C-E)** and P30 **(F-H)** were selectively marked by a CTIP2 antibody. **(C - F)** Representative early-born neuron and cilia images. **(D** and **H)** Histogram of cilia orientation of early-born neurons. (**E - H**) Cilia intracellular localization in four quadrants. There were no changes in cilia orientation and localization from P5 to P30. **(I)** Schematic diagrams depicting cilia orientation and intracellular localization in neocortical principal neurons of WT and *reeler* at P30.

Figure 6. Reelin deficiency partially alters cilia orientation and cilia apical localization in CA1 pyramidal neurons, which undergo postnatal correction. (A-B) Representative neuronal cilia images in the WT (**A**) and *reeler* (**B**) hippocampal CA1 regions at P30. *reeler* CA1 stratum pyramidale (SP) was spitted into two layers, which was named “top” and “bottom”. **(C-D)** Cilia orientation map in WT (**C**) and the top and bottom *reeler* CA1 region (**D**), visualizing cilia orientation across the sampled fields, color-coded by angle (degrees). **(E)** Histogram of cilia orientation in WT CA1 at P30. WT hippocampal neuronal cilia mostly orient toward the pia, with a small fraction toward the ventricular zone. **(F - H)** Histograms showing cilia orientation (0 - 360°) in the top and bottom layers of *reeler* CA1 SP at P10, P14, and P30, respectively. At P10, cilia display broad peaks at ~98° and ~274°, with ~41% and 59% of

cilia oriented in each direction, respectively (**F**). At P14, peaks are observed at ~97° and ~275°, with ~45% and 55% distribution (**G**). By P30, the distribution sharpens, with distinct peaks at ~95° and ~273°, each comprising ~49% and 51% of cilia, respectively (**H**). **(I-K)** Cilia intracellular localization in *reeler* CA1 neurons rectified during postnatal development. Top: Representative examples of WT CA1 neuron cilia of P30 (**I**), *reeler* P10 (**J**) and *reeler* P30 (**K**). Middle: individual neurons and their cilia. Bottom: cilia intracellular localization in four quadrants. The cilia apical localization of *reeler* CA1 neurons increases from ~38% at P10 to ~70% at P30.

Figure 7. Disrupted cilia orientation and apical localization in the *reeler* piriform cortex. (A-D) WT piriform cortex at P30. **(A)** Representative images of Layer II-III and individual examples, with cilia showing a strong directional bias and apical localization. **(B-C)** Histogram of cilia orientation in Layer II and III. Layer II, a compact lamina, exhibited opposite cilia orientation, while Layer III, sparsely laminated, has cilia predominantly oriented toward the pial surface. **(D)** Percentage of cilia/centriole localization in 4 quadrants. Cilia primarily distribute to the apical quadrant. **(E-G)** *reeler* piriform cortex at P30. **(E)** Representative images and individual reeler neurons with cilia lost preferred orientation. **(F)** Histogram of cilia orientation in the *reeler* piriform cortex at P30. We could not distinguish different layers in the *reeler* piriform cortex. inner layer and outer layer of reeler has similar phenotypes. **(G)** Percentage of cilia/centriole localization in 4 quadrants.

Figure 8. Reelin deficiency promotes cilia elongation in principal neurons after P14 throughout the cerebral cortex. (**Left**) Representative images of neuronal primary cilia (marked by an AC3 antibody) in different brain regions of WT and *Reeler* at P14 and P30. (**Right**) Bar graph showing cilia length of

P14 and P30 WT and *reeler* mice. Strongly increased cilia length of principal neurons at P30 but not P14 in various *reeler* cerebral cortex: **(A)** CA1; **(B)** CA3; **(C)** Deep Neocortex; **(D)** Superficial Neocortex; and **(E)** Piriform Cortex.

Supplemental Figure Legends:

Fig. S1. Irregular cilia orientation and random cilia localization in atypical pyramidal neurons in the WT deep neocortex. (A) Representative image of atypical pyramidal neurons stained with NeuN antibody (Top) or Glutaminase II (Bottom). **(B)** Representative cilia images in the deep layer. **(C)** Cilia orientation map of atypical pyramidal neurons visualizing cilia orientation across the sampled fields, color-coded by angle (degrees). Data were pooled from multiple sections out of 3 animals. **(D)** Histogram showing the frequency distribution of cilia orientation angles (0° - 360°), with a flattened fitting curve indicating random orientation. **(E)** Cilia of atypical pyramidal neurons were distributed to 4 quadrants, without a predominant distribution.

Fig. S2. Primary cilia of excitatory neurons in the WT and *reeler* amygdala exhibit random orientation and irregular localization. (A-B) Representative images of excitatory neurons, marked by Glutaminase II antibody, and AC3-marked primary cilia in the amygdala of WT **(A)** and *reeler* **(B). (C-D)** Cilia orientation histogram shows the distribution of cilia orientation angles of excitatory neurons in the amygdala of WT at P30, which reveals a pattern of broad, non-directional orientation. **(D)** WT cilia subcellular localization in 4 quadrants**. (E-F)** Similar cilia orientation and localization patterns were observed in *reeler*. In both genotypes, cilia orientations were distributed across the full 360° range without a dominant axis, indicating random alignment.

Fig. S4. Disrupted layering in the *reeler* DG and CA3. Representative neuron and cilia images, marked by NeuN and AC3 antibodies. Data were collected from P30 mouse brains. Histograms of cilia orientation and cilia intracellular localization in WT and *reeler* are provided in the right two columns. The pattern of cilia orientation and cilia intracellular localization in WT DG and CA3 at P30 were not very strong or difficult to distinguish.

Fig. S3. **Interneurons and astrocytes do not have preferred intracellular localization in soma.** Cilia or centrioles were roughly evenly dispersed to 4 quadrants in WT and *reeler* interneurons and astrocytes, lacking a dominant distribution. **(A)** WT interneurons; **(B)** *reeler* interneurons; **(C)** WT astrocytes; **(D)** *reeler* astrocytes. Interneurons and astrocytes were marked by GAD65 and GFAP antibodies, respectively. Insert, a diagram showing how 4 quadrants in the soma (Top, Bottom, Lateral-Left and Lateral-Right) were defined in reference to the nucleus.

Fig. S5. Reelin does not influence the cilia length of excitatory neurons in non-laminated brain regions. (A) Representative neuronal cilia images and bar graph showing comparable cilia length in the thalamus of WT and *reeler* mice at P30. Similar measurements in the striatum **(B)**, hypothalamus **(C)**, and amygdala **(D)** also showed no significant differences between genotypes. Statistical analysis was performed using Student's T-test. ns, not significant.

Fig. S6. Reelin does not affect the cilia length in interneurons and astrocytes. **(A)** Representative confocal images and individual neurons and **(B-D)** bar graphs showing primary cilia length in interneurons of WT and *reeler* mice at P30. Interneurons were marked by a GAD65 antibody. **(C - D)** Similar measurements in interneurons from the hippocampal CA1 region, deep and superficial neocortex also revealed no significant differences between genotypes. **(E)** Representative confocal images and individual astrocytes and **(F-H)** bar graphs showing primary cilia length in astrocytes of WT and *reeler* mice at P30. Astrocytes were marked by a GFAP antibody. Similar measurements in astrocytes from the hippocampal CA1 region, deep and superficial neocortex also revealed no significant differences between genotypes. Statistical analysis was performed using Student's T-test.

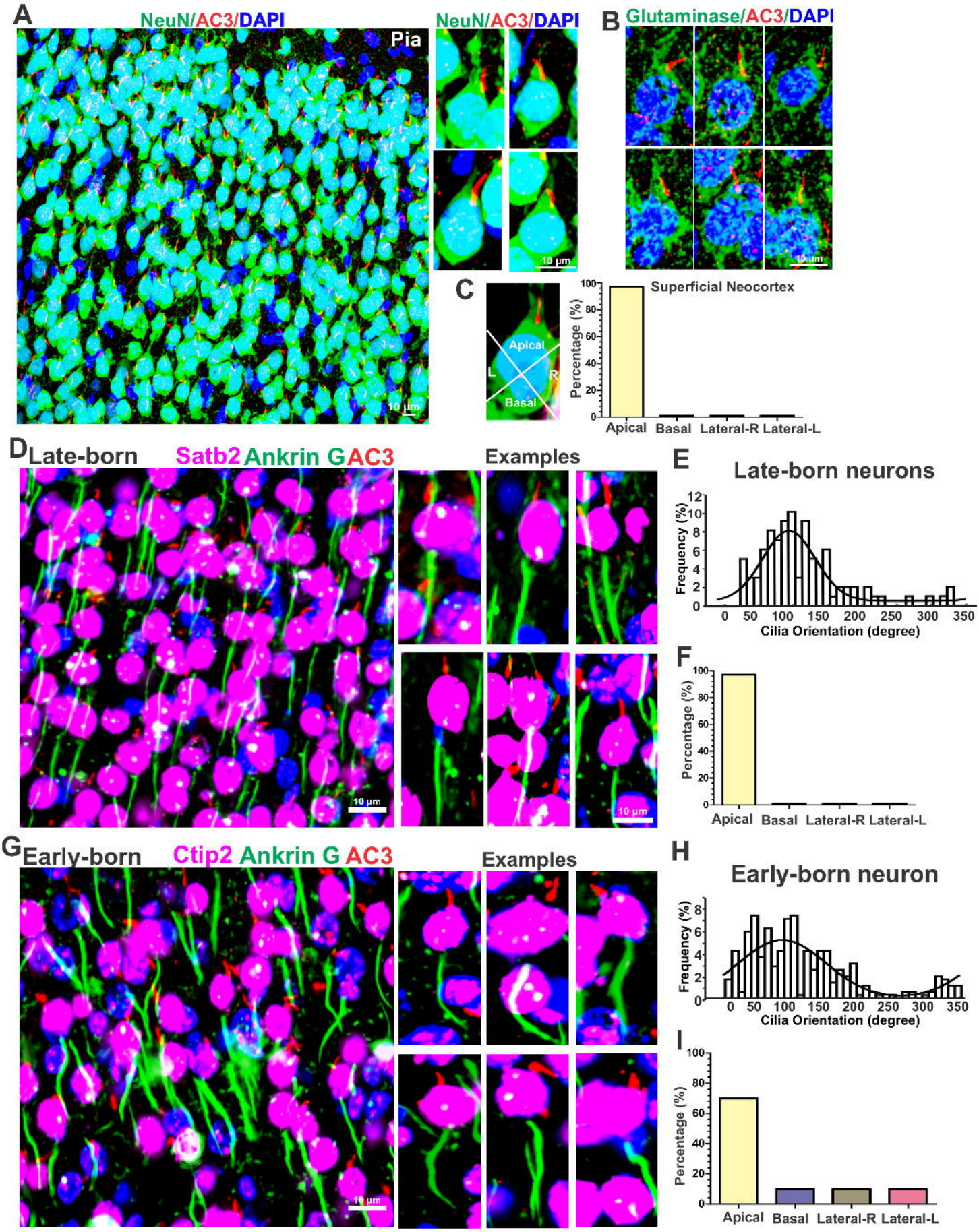
A
NeuN/AC3/DAPI
Pia
10 µm
NeuN/AC3/DAPI
10 µm
B
Glutaminase/AC3/DAPI
10 µm
C
Apical
L
R
Basal
Superficial Neocortex
Percentage (%)
Apical
Basal
Lateral-R
Lateral-L
D
Late-born
Satb2 Ankrin G AC3
Examples
10 µm
10 µm
E
Late-born neurons
Frequency (%)
Cilia Orientation (degree)
F
Percentage (%)
Apical
Basal
Lateral-R
Lateral-L
G
Early-born
Ctip2 Ankrin G AC3
Examples
10 µm
H
Early-born neuron
Frequency (%)
Cilia Orientation (degree)
I
Percentage (%)
Apical
Basal
Lateral-R
Lateral-L

Figure 1

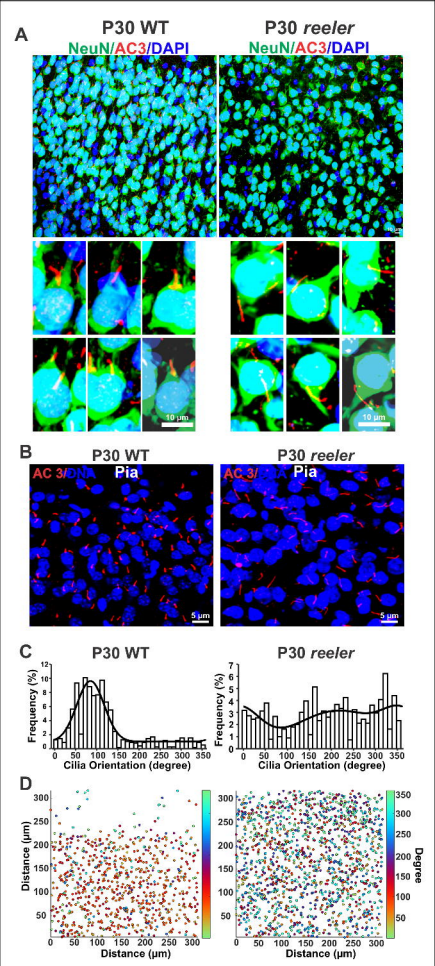
A
P30 WT
NeuN/AC3/DAPI
P30 reeler
NeuN/AC3/DAPI
10 µm
10 µm
B
P30 WT
AC 3/DNA
Pia
5 µm
P30 reeler
AC 3/DNA
Pia
5 µm
C
P30 WT
Frequency (%)
Cilia Orientation (degree)
P30 reeler
Frequency (%)
Cilia Orientation (degree)
D
Distance (µm)
Distance (µm)
Distance (µm)
Distance (µm)
Degree

Figure 2

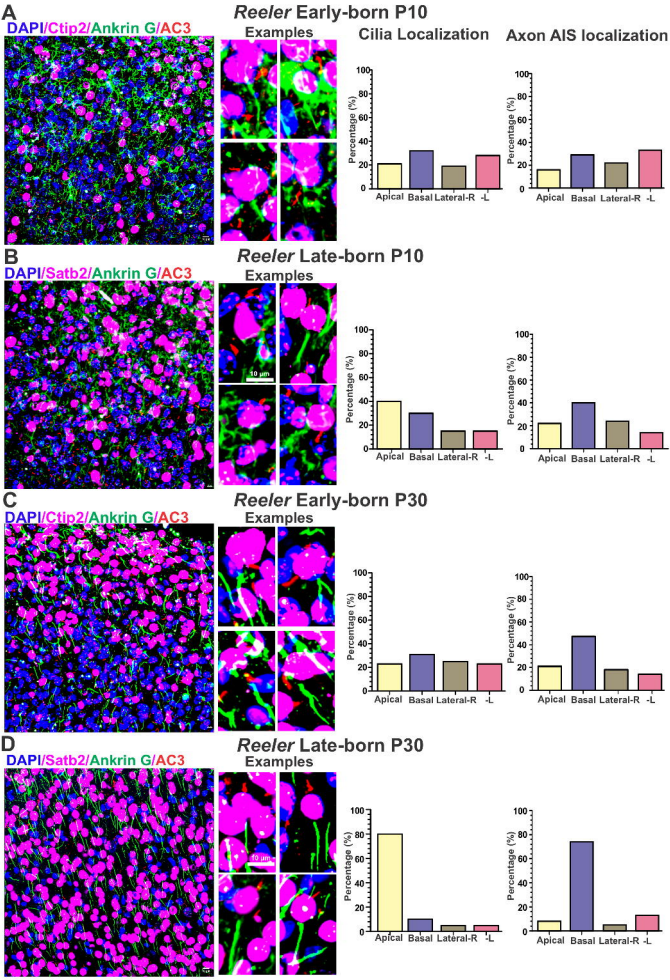
A
Reeler Early-born P10
DAPI/Ctip2/Ankrin G/AC3
Examples
Cilia Localization
Axon AIS localization
Percentage (%)
Apical
Basal
Lateral-R
-L
B
Reeler Late-born P10
DAPI/Satb2/Ankrin G/AC3
Examples
10 µm
C
Reeler Early-born P30
DAPI/Ctip2/Ankrin G/AC3
Examples
D
Reeler Late-born P30
DAPI/Satb2/Ankrin G/AC3
Examples

Figure 3

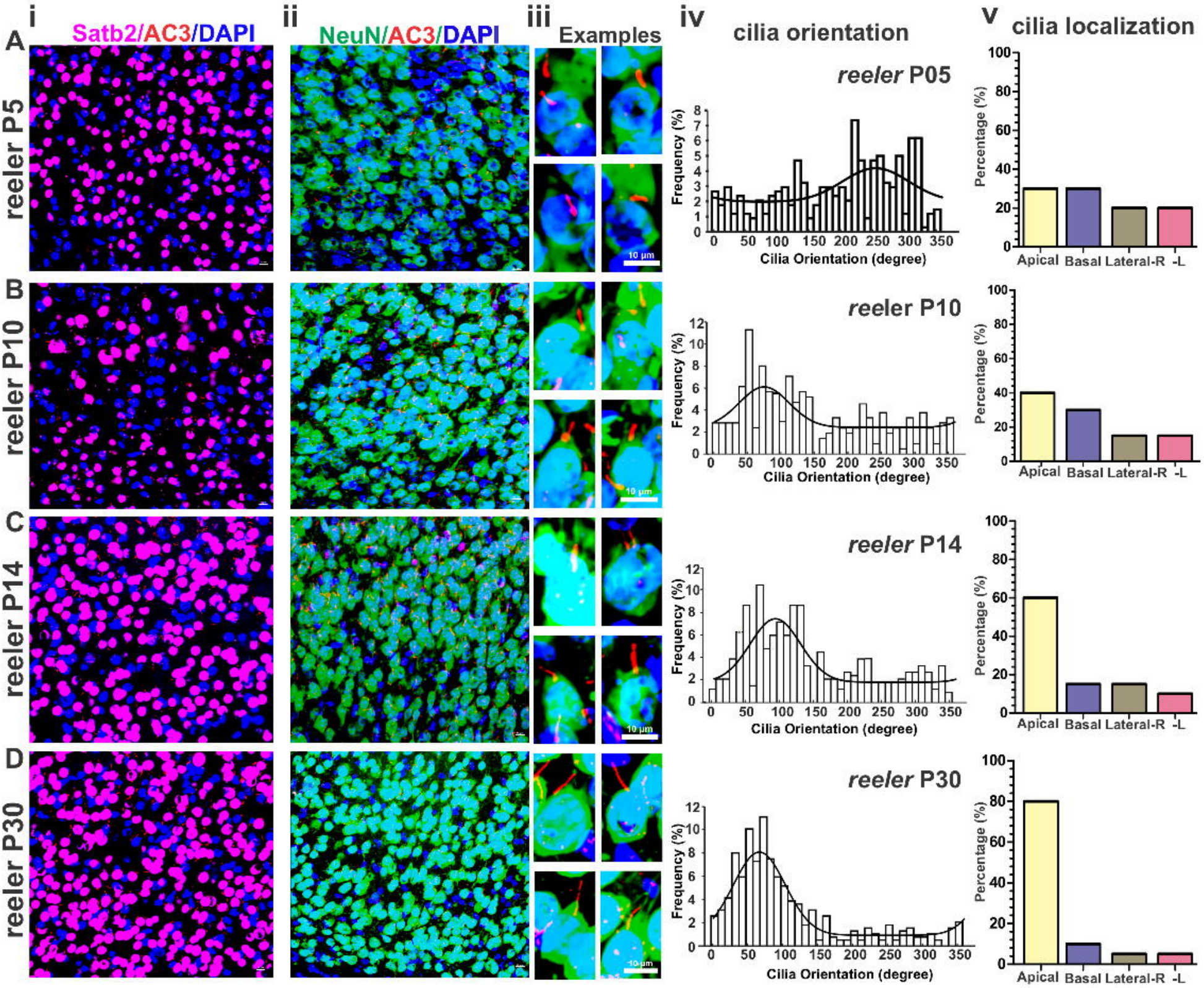
i
Satb2/AC3/DAPI
ii
NeuN/AC3/DAPI
iii
Examples
iv
cilia orientation
v
cilia localization
A
reeler P5
B
reeler P10
C
reeler P14
D
reeler P30
10 µm
Frequency (%)
Cilia Orientation (degree)
Percentage (%)
Apical
Basal
Lateral-R
-L

Figure 4

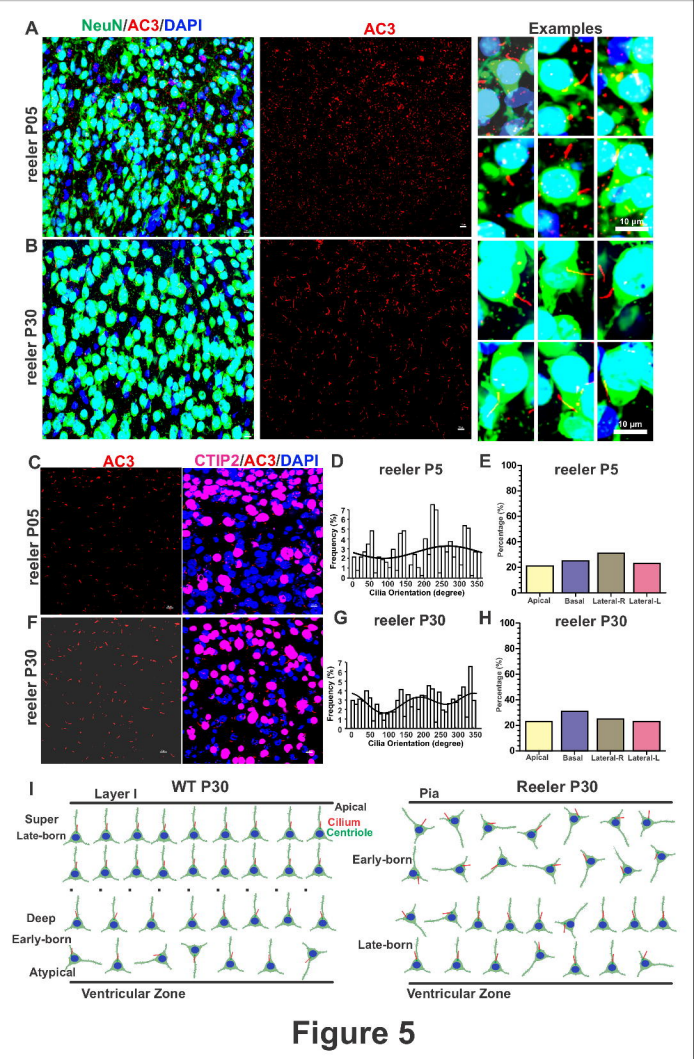
A
NeuN/AC3/DAPI
AC3
Examples
reeler P05
B
reeler P30
10 µm
C
AC3
CTIP2/AC3/DAPI
reeler P05
D
reeler P5
Frequency (%)
Cilia Orientation (degree)
E
reeler P5
Percentage (%)
Apical
Basal
Lateral-R
Lateral-L
F
reeler P30
G
reeler P30
H
reeler P30
I
Layer I
WT P30
Apical
Cilium
Centriole
Super
Late-born
Deep
Early-born
Atypical
Ventricular Zone
Pia
Reeler P30
Early-born
Late-born
Ventricular Zone

Figure 5

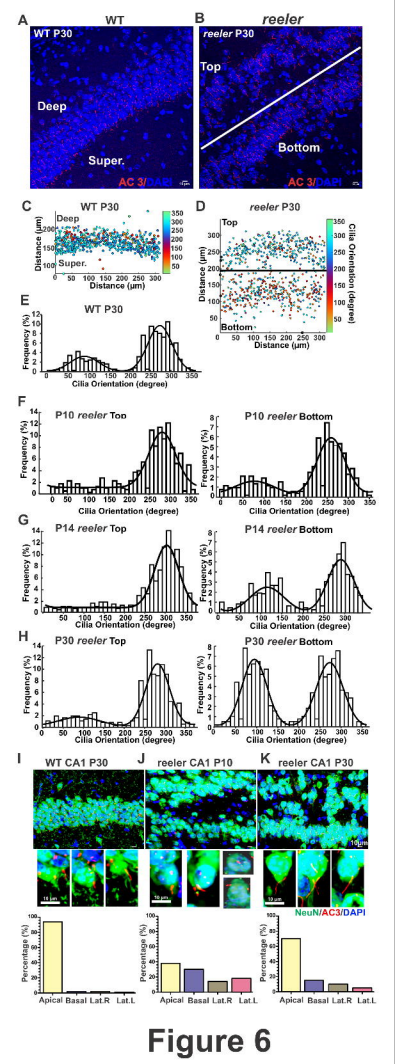
A
WT
WT P30
Deep
Super.
AC 3/DAPI
B
reeler
reeler P30
Top
Bottom
AC 3/DAPI
C
WT P30
Deep
Super.
Distance (μm)
D
reeler P30
Top
Bottom
Cilia Orientation (degree)
E
WT P30
Frequency (%)
Cilia Orientation (degree)
F
P10 reeler Top
P10 reeler Bottom
G
P14 reeler Top
P14 reeler Bottom
H
P30 reeler Top
P30 reeler Bottom
I
WT CA1 P30
J
reeler CA1 P10
K
reeler CA1 P30
NeuN/AC3/DAPI
Percentage (%)
Apical
Basal
Lat.R
Lat.L

Figure 6

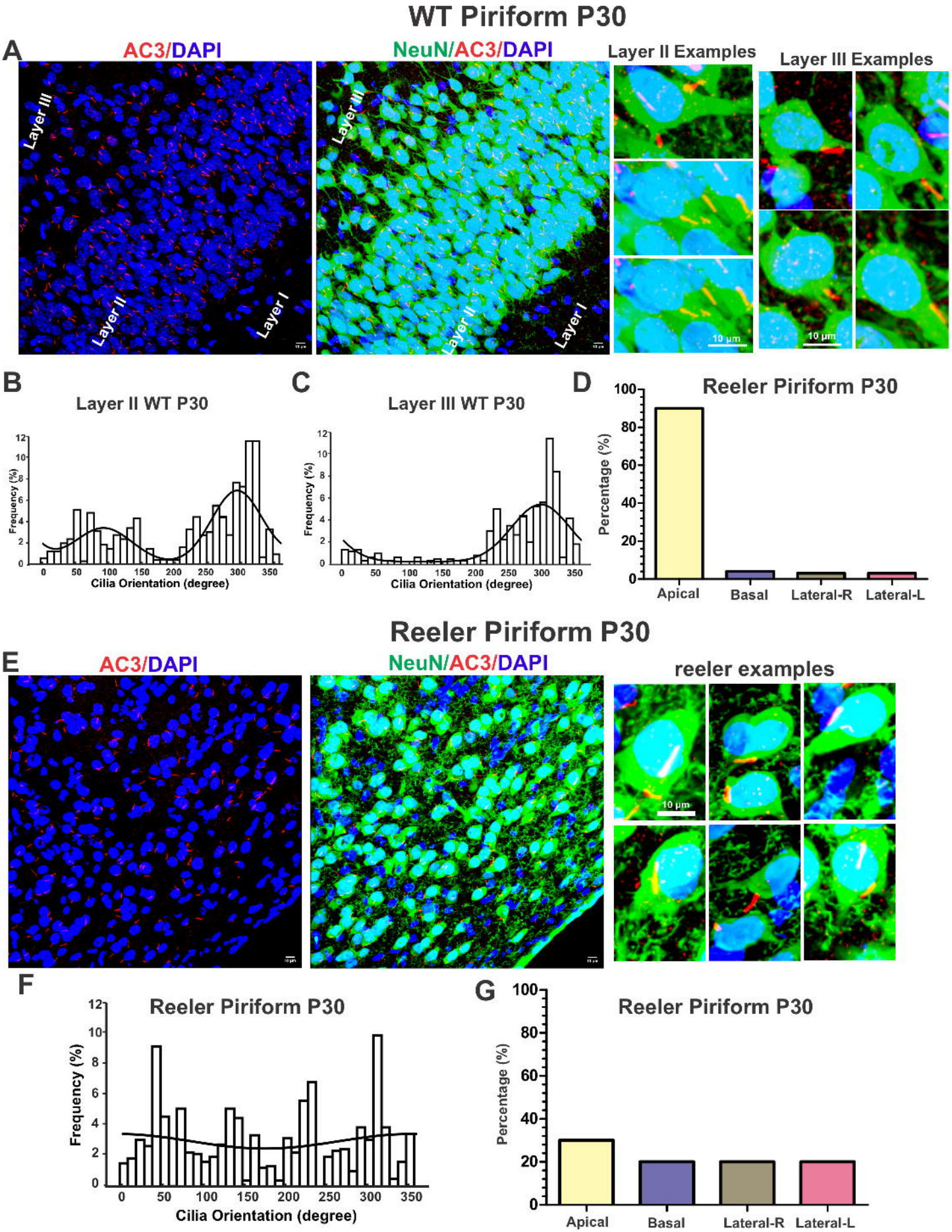
WT Piriform P30
A
AC3/DAPI
NeuN/AC3/DAPI
Layer II Examples
Layer III Examples
Layer III
Layer II
Layer I
10 µm
B
Layer II WT P30
Frequency (%)
Cilia Orientation (degree)
C
Layer III WT P30
D
Reeler Piriform P30
Percentage (%)
Apical
Basal
Lateral-R
Lateral-L
Reeler Piriform P30
E
AC3/DAPI
NeuN/AC3/DAPI
reeler examples
F
Reeler Piriform P30
Frequency (%)
Cilia Orientation (degree)
G
Reeler Piriform P30
Percentage (%)
Apical
Basal
Lateral-R
Lateral-L

Figure 7

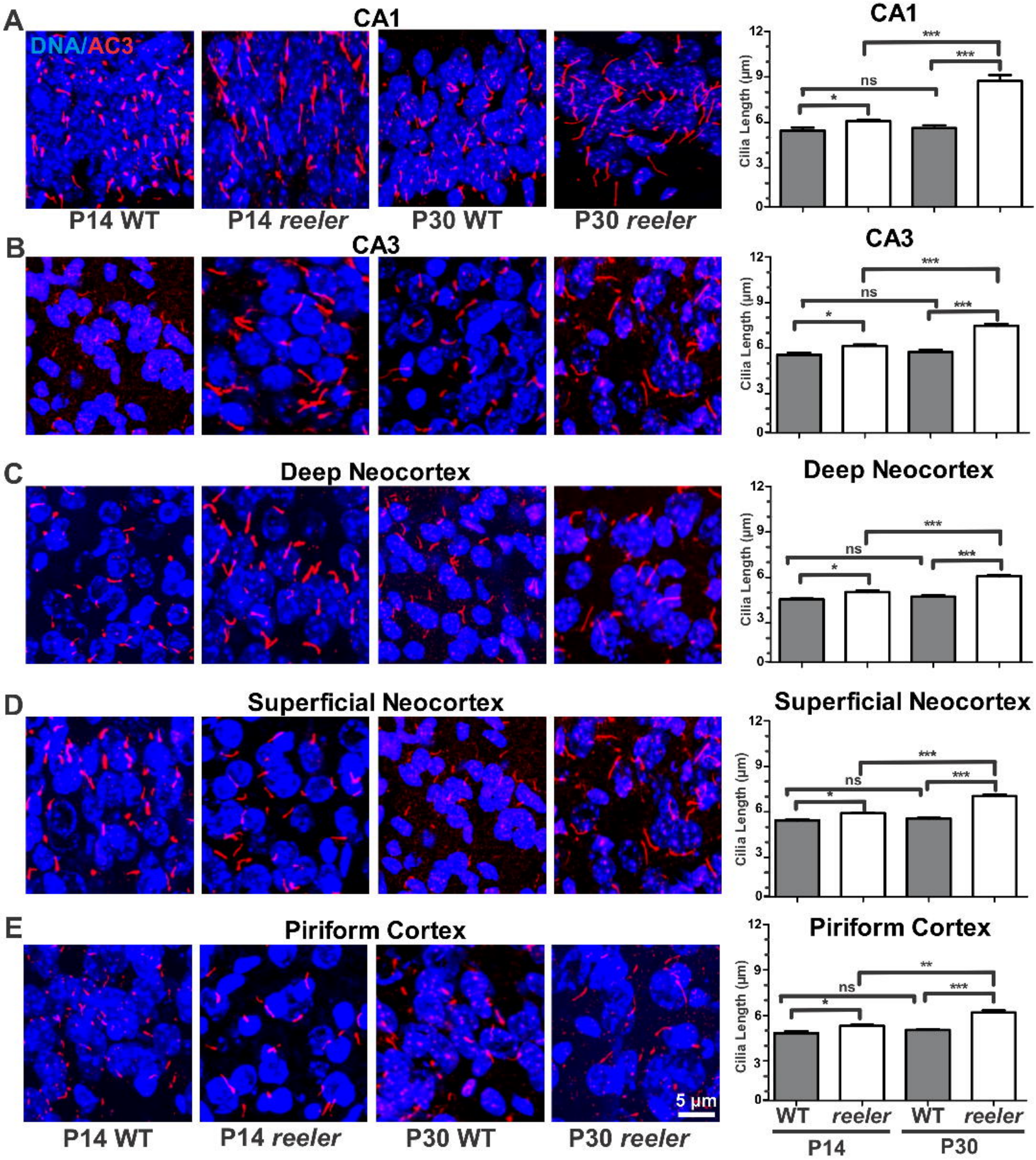
A
CA1
DNA/AC3
P14 WT
P14 reeler
P30 WT
P30 reeler
CA1
Cilia Length (µm)
ns
*
***
***
B
CA3
CA3
C
Deep Neocortex
Deep Neocortex
D
Superficial Neocortex
Superficial Neocortex
E
Piriform Cortex
Piriform Cortex
5 µm
WT
reeler
WT
reeler
P14
P30

Figure 8

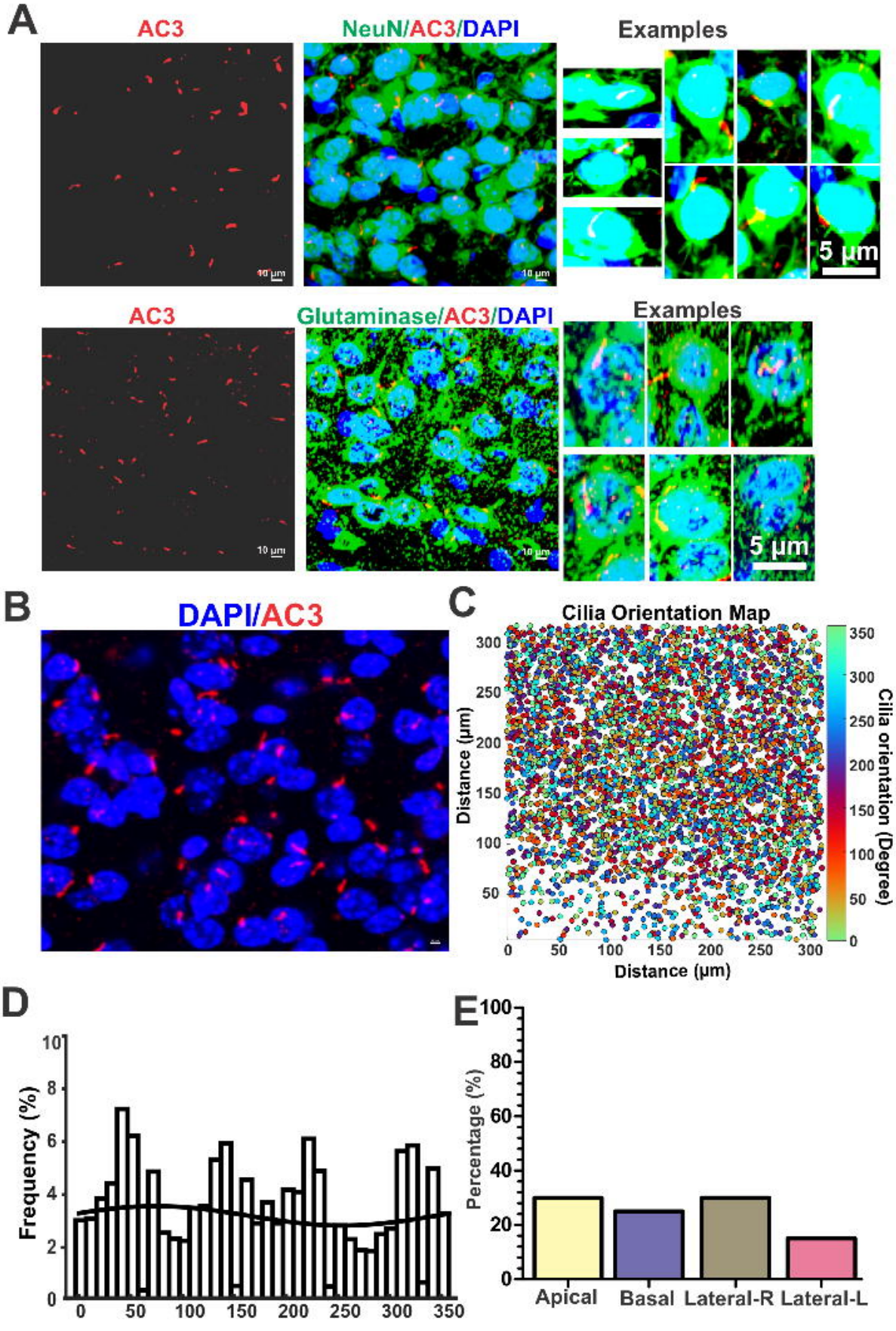
A
AC3
NeuN/AC3/DAPI
Examples
10 µm
5 µm
AC3
Glutaminase/AC3/DAPI
Examples
10 µm
5 µm
B
DAPI/AC3
C
Cilia Orientation Map
Distance (µm)
Distance (µm)
Cilia orientation (Degree)
D
Frequency (%)
E
Percentage (%)
Apical
Basal
Lateral-R
Lateral-L

Fig. S1

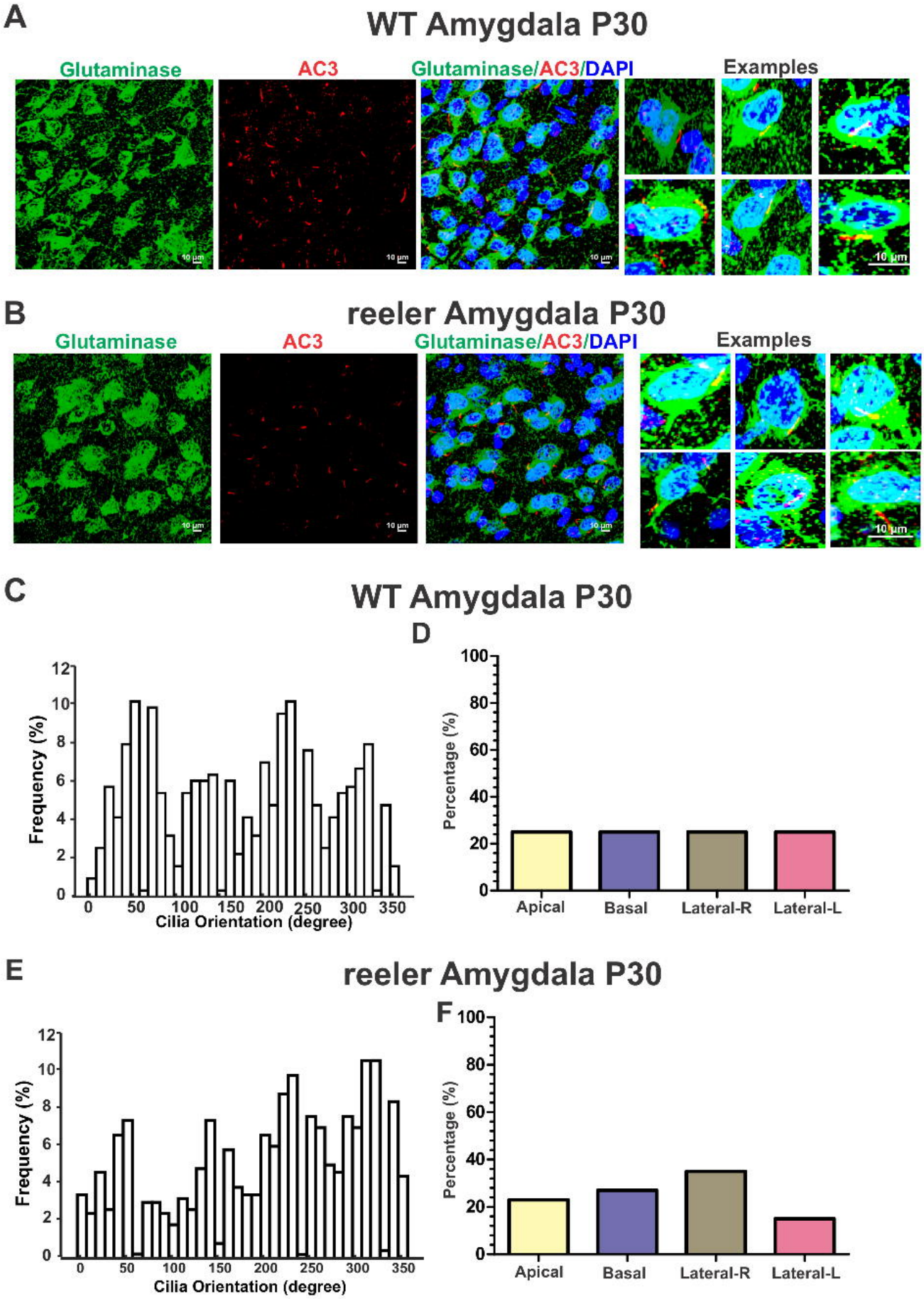
A
WT Amygdala P30
Glutaminase
AC3
Glutaminase/AC3/DAPI
Examples
10 µm
B
reeler Amygdala P30
Glutaminase
AC3
Glutaminase/AC3/DAPI
Examples
10 µm
C
WT Amygdala P30
Frequency (%)
Cilia Orientation (degree)
D
Percentage (%)
Apical
Basal
Lateral-R
Lateral-L
E
reeler Amygdala P30
Frequency (%)
Cilia Orientation (degree)
F
Percentage (%)
Apical
Basal
Lateral-R
Lateral-L

Fig. S2

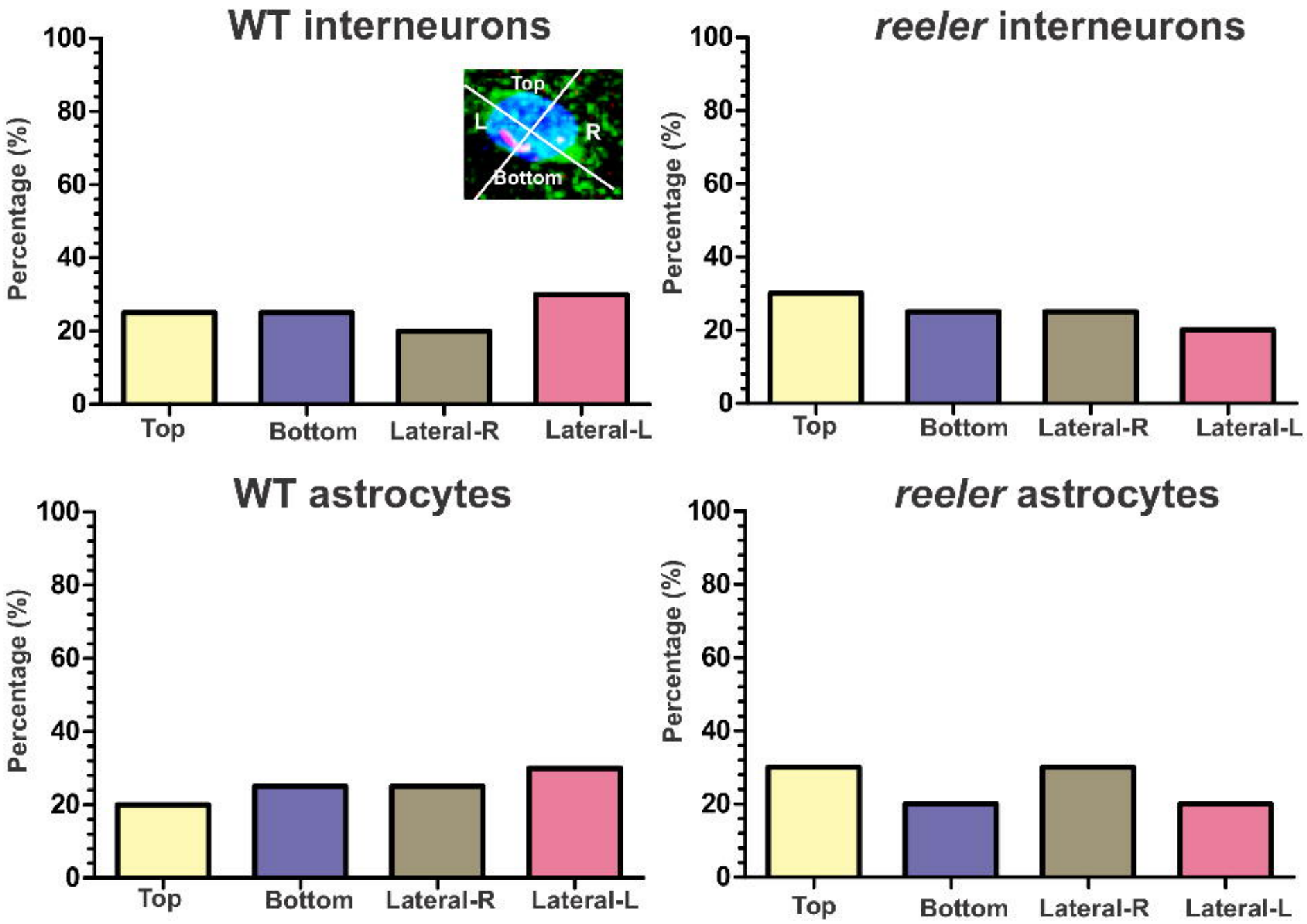
WT interneurons
Percentage (%)
100
80
60
40
20
0
Top
Bottom
L
R
Top
Bottom
Lateral-R
Lateral-L
reeler interneurons
Percentage (%)
Top
Bottom
Lateral-R
Lateral-L
WT astrocytes
Percentage (%)
Top
Bottom
Lateral-R
Lateral-L
reeler astrocytes
Percentage (%)
Top
Bottom
Lateral-R
Lateral-L

Fig. S3

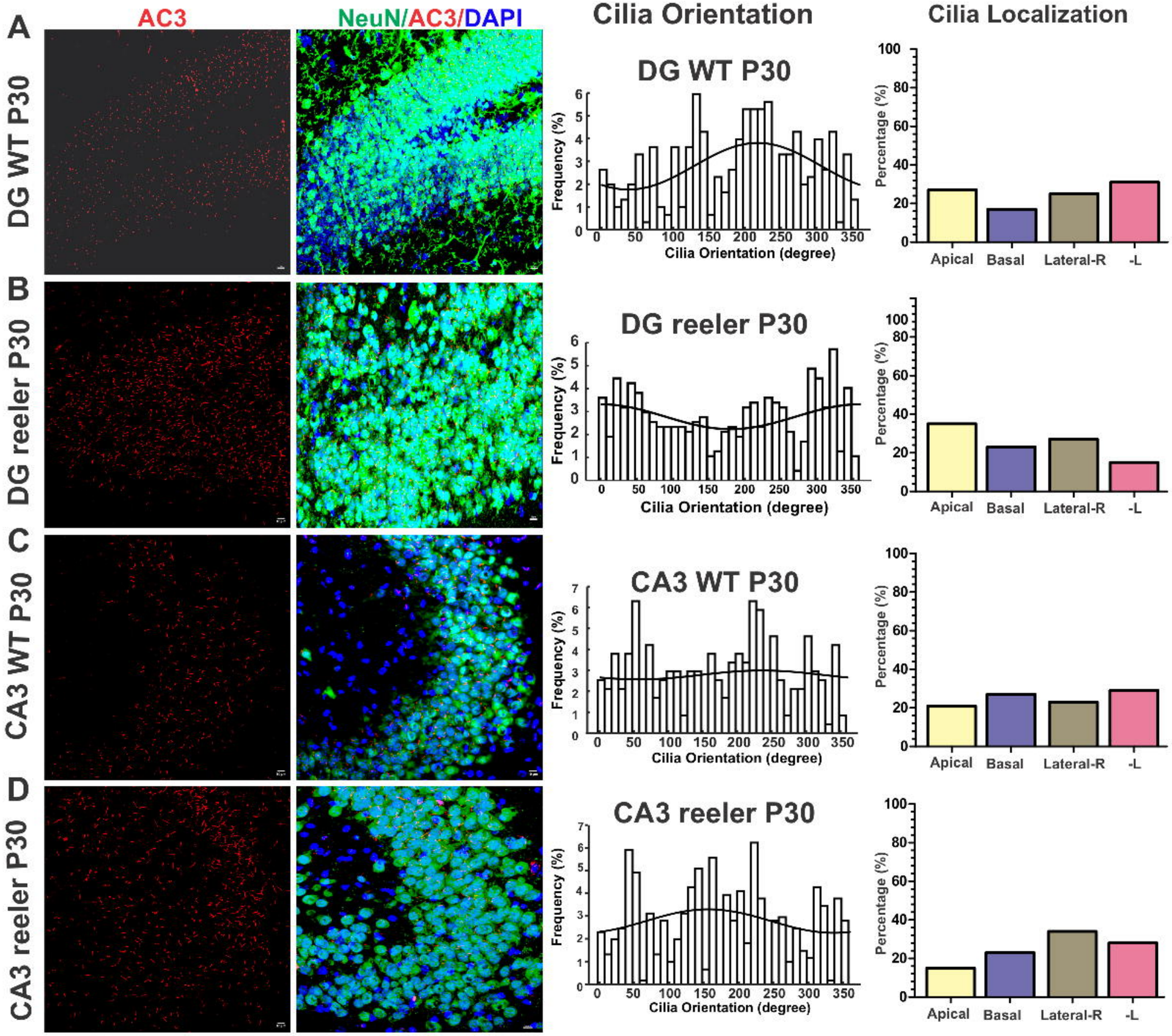
A
B
C
D
AC3
NeuN/AC3/DAPI
Cilia Orientation
Cilia Localization
DG WT P30
DG reeler P30
CA3 WT P30
CA3 reeler P30
Frequency (%)
Cilia Orientation (degree)
Percentage (%)
Apical
Basal
Lateral-R
-L

Fig. S4

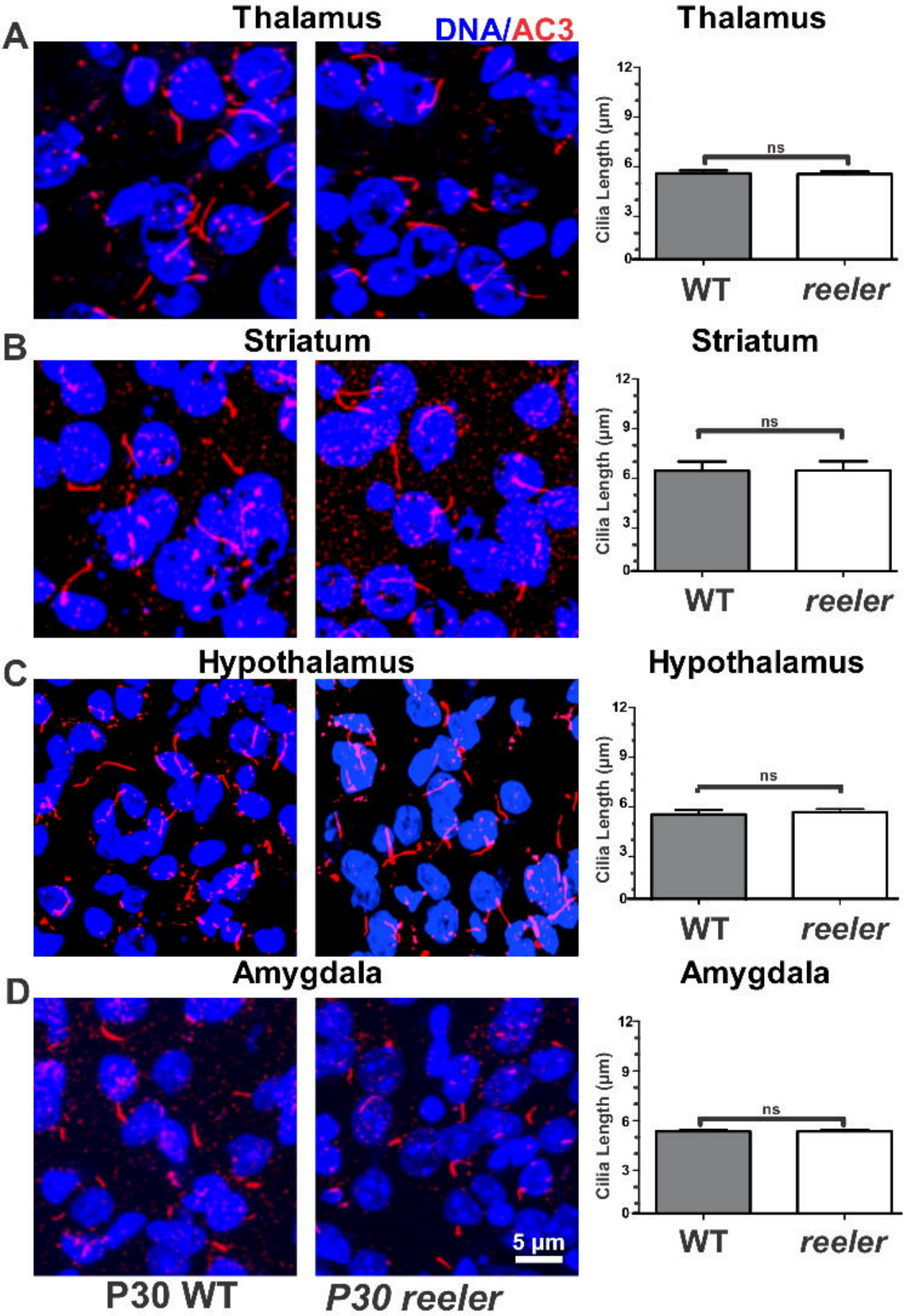
A
Thalamus
DNA/AC3
Thalamus
Cilia Length (µm)
12
9
6
3
0
ns
WT
reeler
B
Striatum
Striatum
Cilia Length (µm)
ns
WT
reeler
C
Hypothalamus
Hypothalamus
Cilia Length (µm)
ns
WT
reeler
D
Amygdala
Amygdala
Cilia Length (µm)
ns
WT
reeler
5 µm
P30 WT
P30 reeler

Fig. S5

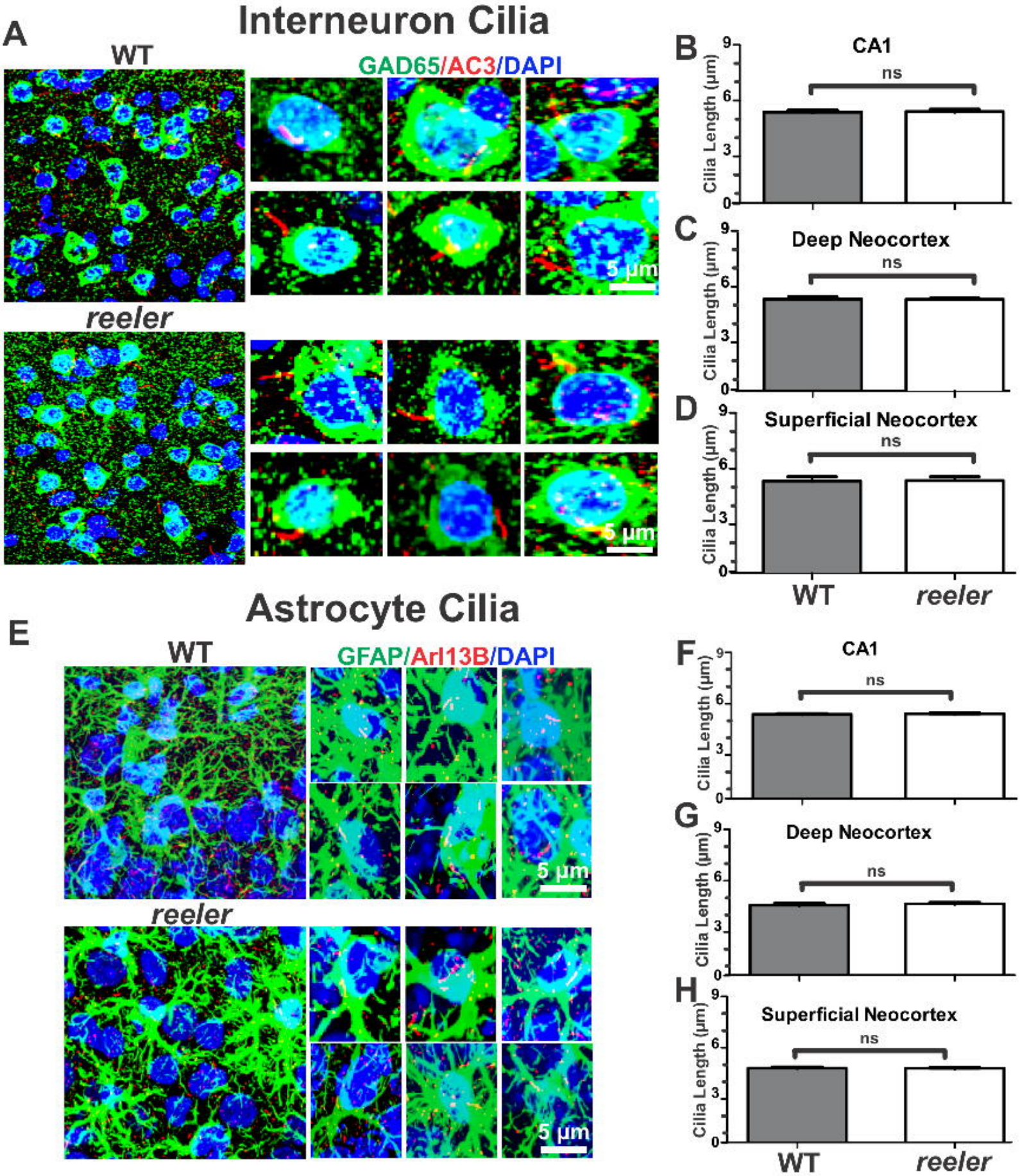
A
Interneuron Cilia
WT
GAD65/AC3/DAPI
5 µm
reeler
5 µm
B
CA1
ns
Cilia Length (µm)
C
Deep Neocortex
ns
Cilia Length (µm)
D
Superficial Neocortex
ns
Cilia Length (µm)
WT
reeler
E
Astrocyte Cilia
WT
GFAP/Arl13B/DAPI
5 µm
reeler
5 µm
F
CA1
ns
Cilia Length (µm)
G
Deep Neocortex
ns
Cilia Length (µm)
H
Superficial Neocortex
ns
Cilia Length (µm)
WT
reeler

Fig. S6